

UC Irvine

UC Irvine Previously Published Works

Title

RAR β 2 is required for vertebrate somitogenesis

Permalink

<https://escholarship.org/uc/item/8qc4s7cf>

Journal

Development, 144(11)

ISSN

0950-1991

Authors

Janesick, Amanda
Tang, Weiyi
Nguyen, Tuyen TL
[et al.](#)

Publication Date

2017-06-01

DOI

10.1242/dev.144345

Copyright Information

This work is made available under the terms of a Creative Commons Attribution-NonCommercial-NoDerivatives License, available at <https://creativecommons.org/licenses/by-nc-nd/4.0/>

Peer reviewed

RESEARCH ARTICLE

RAR β 2 is required for vertebrate somitogenesisAmanda Janesick^{1,*}, Weiyi Tang^{1,‡}, Tuyen T. L. Nguyen¹ and Bruce Blumberg^{1,2,§}

ABSTRACT

During vertebrate somitogenesis, retinoic acid is known to establish the position of the determination wavefront, controlling where new somites are permitted to form along the anteroposterior body axis. Less is understood about how RAR regulates somite patterning, rostral-caudal boundary setting, specialization of myotome subdivisions or the specific RAR subtype that is required for somite patterning. Characterizing the function of RAR β has been challenging due to the absence of embryonic phenotypes in murine loss-of-function studies. Using the *Xenopus* system, we show that RAR β 2 plays a specific role in somite number and size, restriction of the presomitic mesoderm anterior border, somite chevron morphology and hypaxial myoblast migration. *Rarb2* is the RAR subtype whose expression is most upregulated in response to ligand and its localization in the trunk somites positions it at the right time and place to respond to embryonic retinoid levels during somitogenesis. RAR β 2 positively regulates *Tbx3* a marker of hypaxial muscle, and negatively regulates *Tbx6* via *Ripply2* to restrict the anterior boundaries of the presomitic mesoderm and caudal progenitor pool. These results demonstrate for the first time an early and essential role for RAR β 2 in vertebrate somitogenesis.

KEY WORDS: Retinoic acid receptor β 2, *Ripply2*, Somitogenesis, Hypaxial muscle

INTRODUCTION

The vertebrate retinoic acid receptor (RAR) family comprises three genes encoding three RAR subtypes: RAR α , RAR β and RAR γ . These subtypes differ in their temporal and spatial expression, inducibility by retinoic acid (RA) (auto-regulation), post-translational modification, epigenetic regulation and basal repression (e.g. co-factor recruitment). It is posited that certain vertebrate innovations (neural crest, sensory placodes, segmentation of the brain, etc.) necessitated the evolution of the three RAR subtypes that subspecialized to modulate diverse developmental processes (Albalat et al., 2011). The ligand binding domain of an inferred ancestral RAR most closely resembles mammalian RAR β , which is considered to be the most primitive of RARs. Therefore, RAR β was likely to be the first RAR to evolve (Escriva et al., 2006).

One obstacle to studying the different roles of RAR subtypes is the lack of embryonic phenotypes observed in mouse RAR knockout studies. For example, disruption of murine RAR β 2 led

to mostly non-embryonic, adult phenotypes such as deficits in memory/spatial skills, premature alveolus formation (Massaro et al., 2000; Chiang et al., 1998), impaired growth, increased proliferation and pigmentation behind the lens, and occasional vertebral homeotic transformations (Ghyselinck et al., 1997). *Rara*^{-/-} embryos are viable up until 2 months after birth (Lufkin et al., 1993; Massaro et al., 2003). Only double subtype mutants (e.g. *Rarb/Rarg*^{-/-}, *Rara/Rarg*^{-/-}) yield overt embryonic phenotypes (Lohnes et al., 1994; Subbarayan et al., 1997, reviewed by Maden, 2010). This apparent functional redundancy may not represent the physiological condition, but rather an incomplete exploration of the possible phenotypes in the laboratory environment (Mark et al., 2006; Ghyselinck et al., 1997). Indeed, *Rarb*^{-/-} mice do not develop microphthalmia (Ghyselinck et al., 1997), as observed in humans with RAR β loss of function (Srouf et al., 2013). Aside from oncogenic fusions (e.g. PML-RAR α , RAR γ /NUP98), there are no reported mutations for human RAR α or RAR γ associated with diseases (<http://omim.org>), suggesting that such mutations may be embryonic lethal. This provides evidence that human RARs generally cannot compensate for each other, and that mouse might not be an ideal model for studying the function of individual RAR subtypes.

In chick and zebrafish, loss of individual RARs causes specific phenotypes (Romeih et al., 2003; Garnaas et al., 2012; He et al., 2011; D'Aniello et al., 2013). RAR α or RAR γ knockdown in the frog, *Xenopus laevis*, produces specific defects in neuronal differentiation, pre-placodal ectoderm formation and axial elongation (Janesick et al., 2014, 2013, 2012; Koide et al., 2001). We have shown that RAR γ is required for axial elongation and for maintenance of the caudal progenitor pool (Janesick et al., 2014). However, RAR γ is mostly absent from the trunk and lateral plate mesoderm from which RA emanates. Therefore, RA-regulated processes such as neural tube patterning, hindbrain boundary setting, somite differentiation, limb development, and heart and lung morphogenesis (Maden, 2007; Niederreither and Dollé, 2008) likely rely on RAR α or RAR β . Although RAR β is expressed in the somites and lateral plate mesoderm, positioning it to regulate somitogenesis in chick and mouse (Cui et al., 2003; Ruberte et al., 1991; Romeih et al., 2003; Bayha et al., 2009), the functionality of RAR β in early somitic development had not been explored.

Somitogenesis is a process whereby cells from the caudal progenitor pool contribute to the presomitic mesoderm (PSM) that contains committed somite precursor cells to supply the rostral, determination wavefront (reviewed by Dequéant and Pourquié, 2008). The decision of cells within the caudal progenitor pool to become PSM is restricted by an alternative, mutually exclusive fate decision towards the elongating neural tube, indicated by *Sox2* expression (Takemoto et al., 2011). The PSM is initially homogenous, marked by *Mesogenin1* and *Tbx6*, then gradually organizes into a mesenchymal mass patterned as somitomeres (newly forming somites) (Dequéant and Pourquié, 2008) marked by genes such as *Mespa* and *Ripply2*. *Tbx6* promotes somite maturation (Nikaido et al., 2002) and its targets are repressed by

¹Department of Developmental and Cell Biology, 2011 Biological Sciences 3, University of California, Irvine, CA 92697-2300, USA. ²Department of Pharmaceutical Sciences, University of California, Irvine, CA 92697, USA. ^{*}Present address: Department of Otolaryngology – Head & Neck Surgery, Stanford University School of Medicine, Stanford, CA 94305, USA. [‡]Present address: Division of Biology, California Institute of Technology, Pasadena, CA 91125, USA.

[§]Author for correspondence (blumberg@uci.edu)

 A.J., 0000-0001-7731-2756; B.B., 0000-0002-8016-8414

Ripply2 to facilitate establishment of somite boundaries (Dahmann et al., 2011). Epithelialization of the somitomeres produces mature somites (Nakaya et al., 2004), which are dorsoventrally segregated into epaxial and hypaxial territories (Cheng et al., 2004). Hypaxial dermomyotome cells ultimately delaminate and migrate to populate musculature in the limb, diaphragm and tongue (Dietrich et al., 1998; Martin and Harland, 2001).

Considering that knockdown of individual *Xenopus* RAR subtypes or isoforms yields distinct embryonic phenotypes, we characterized the role of RAR β 2 in somitogenesis. Here, we show that expression of *Rar β 2* is induced by the RAR agonist TTNPB, and diminished by the RAR antagonist AGN193109 due to the presence of two highly conserved RA response elements (RAREs) in the promoter of *Rar β 2*. *Rar β 2* is the last RAR subtype to be expressed during *Xenopus* development. We hypothesize that other RAR subtypes are required to initiate or maintain *Rar β 2* expression because knockdown of either RAR α or RAR γ ablates *Rar β 2* expression. RAR β 2 is spatially positioned to be the subtype most responsive to ligand emanating from the trunk, and is required to restrict PSM markers. Loss of RAR β 2 yields a multifaceted phenotype on somitogenesis: somite number is decreased and domains are larger, chevron morphology is perturbed, and hypaxial myoblasts fail to migrate ventrally. We also explored the *in vivo* transcriptional relationships between *Ripply2*, an RAR-responsive gene that regulates boundary setting during somitogenesis, *Tbx6* (a PSM marker) and *Tbx3* (a hypaxial myoblast and notochord marker). We found that *Ripply2* inhibits *Tbx6* transcriptional activity, while the ability of *Tbx3* to repress transcription does not involve *Ripply2*. Taken together, our results show for the first time that RAR β 2 plays an early and important role in somitogenesis.

RESULTS

RAR β 2 is the predominant RAR β isoform in *Xenopus laevis*

Using the latest genome assembly available for *X. laevis* (build 9.1) (Session et al., 2016), we identified *Rar β 1* and *Rar β 2* via comparison with *X. tropicalis* and submitted these sequences to NCBI (*Rar β 1*, KF547939; *Rar β 2*, KF547940). RAR β is found on chromosome 6, with homeolog copies *Rar β .L* and *Rar β .S* (Session et al., 2016). Fig. S1 demonstrates that *Rar β 1* and *Rar β 2* are isoforms, and differ by alternative promoter usage creating a distinct N-terminal structure, as is the case in mouse, chicken and other vertebrates (Zelent et al., 1991; Leroy et al., 1991; Brand et al., 1990). We mapped the 5' UTRs of *Rar β 1* and *Rar β 2* from *X. tropicalis* to *X. laevis*, and designed antisense RNA probes that could distinguish between the two isoforms (Table S1). Whole-mount *in situ* hybridization determined the temporal and spatial expression of *X. laevis* *Rar β 1* and *Rar β 2* (Fig. 1). *Rar β 1* is not detected by whole-mount *in situ* hybridization at any stage tested (tailbud stage shown in Fig. 1C). *Rar β 2* first exhibits a specific expression pattern at mid-tailbud (approximately stage 26), when it is expressed in mature somites, eye, branchial arches, anterior neural tube and hatching gland (Fig. 1A,B). These data mostly agree with previous *Xenopus* expression data using a partial sequence (Escriva et al., 2006). A sense probe for *Rar β 2* revealed no specific expression, confirming the specificity of our probe (not shown).

QPCR analysis was conducted with primers that amplify both homeologs of either *Rar β 1* or *Rar β 2* (Table S3). A comprehensive, quantitative comparison of all *X. laevis* RAR subtypes and isoforms is shown in Fig. S2. *Rar β 1* is not robustly detected by QPCR until stage 40 (Fig. 1D), which is concordant with whole-mount *in situ* hybridization results. *Rar β 2* is detected at stage 18 by QPCR (Fig. 1D), but does not exhibit distinct expression by whole-mount

in situ hybridization at that stage. Although both *Rar β 1* and *Rar β 2* are maternal transcripts, *Rar β 2* is the predominant *Rar β* isoform expressed during early development. *Rar β 2* mRNA is ~1000-7000 times less abundant than *Rar γ 2* and ~60-1000 times less abundant than *Rara1* and *Rara2* mRNAs at gastrula and neurula stages 10-18 (Fig. S2). At later stages, *Rar β 2* is ~10-100 times less abundant than *Rara1*, *Rara2* and *Rar γ 2* (Fig. S2).

RAR β 2 can be induced by RA, and RAR α 2 and RAR γ 2 are required for *Rar β 2* expression

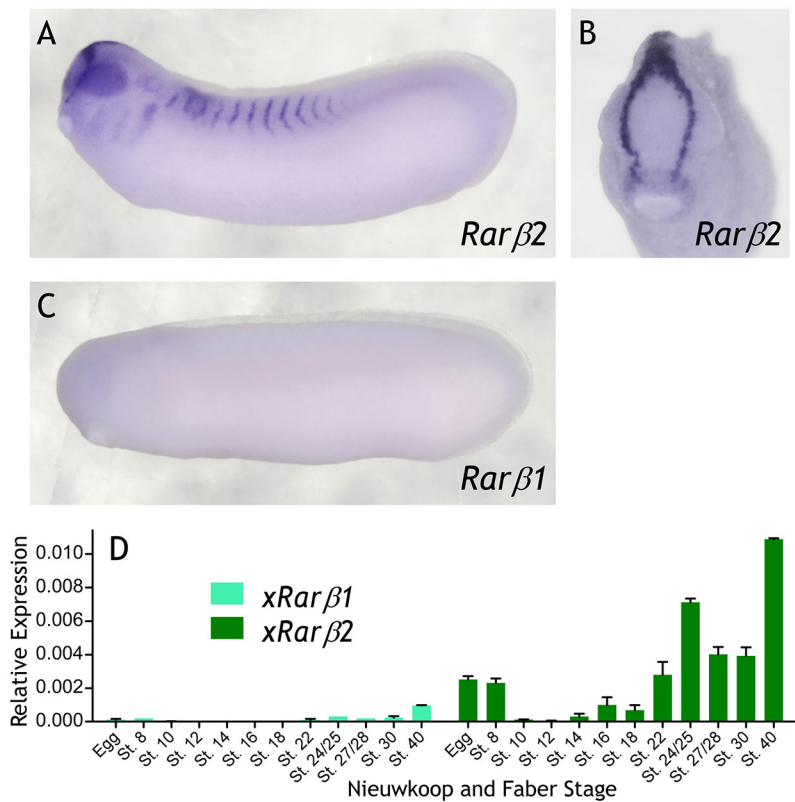
Vertebrate RARs possess RAREs in their regulatory regions and one or more isoforms are directly regulated by RA at the transcriptional level. The first characterized RAREs were identified in the human (de The et al., 1990) and mouse (Sucov et al., 1990) *Rar β 2* promoters. We found that the archetypal 'canonical' RARE, a direct repeat separated by five nucleotides (DR5), is located ~500 bp upstream of the *Rar β 2* start codon and is highly conserved in vertebrates (Fig. S3). In the ascidian, *Ciona intestinalis*, a DR2 RARE is found in the first intron of CiRAR. Inspection of the aligned promoter sequences revealed an additional conserved element in vertebrates composed of an upstream DR5 and an additional conserved half site (Fig. S3). Unlike other vertebrates, zebrafish lacks a recognizable *Rar β* gene. Instead, the RARE is found in *raraa*, an ortholog of *Rar α* (Hale et al., 2006; Waxman and Yelon, 2007), which was reported to be the only RA-inducible zebrafish RAR (Linville et al., 2009). A putative RARE is found upstream of a *Fugu rubripes* gene model labeled 'RAR γ -A-like', which a BLASTP search indicates is most closely related to RAR β (not shown).

The identification of an RARE in both homeologs of *X. laevis* *Rar β 2*, led us to hypothesize that *Rar β 2* is RA inducible, as in other vertebrates. We asked which *Xenopus* RAR subtypes and isoforms responded to the RAR-selective agonist TTNPB, or to the RAR-selective antagonist AGN193109 (Koide et al., 2001). *Rar β 2* is strongly upregulated by TTNPB and repressed by AGN193109 (Fig. 2A). *Rara* isoforms are modestly induced by TTNPB and repressed by AGN193109, *Rar γ 2* is downregulated by TTNPB and *Rar β 1* is not detected by QPCR (Fig. 2A). Furthermore, the expression domain of *Rar β 2* is greatly expanded by TTNPB, particularly in the anterior neural tube and branchial arches (Fig. S4). Knockdown of either RAR α or RAR γ results in loss of *Rar β* expression (Fig. 2B). Hence, *Rara2* and *Rar γ 2*, which are expressed earlier than *Rar β 2* (Fig. S2), are required to initiate or maintain *Rar β 2* expression.

We hypothesized that elements of the *Rar β 2* promoter are required for RA responsiveness and are occupied by RARs. Although the canonical RARE had previously been characterized (Fig. S3), the other conserved elements had not. We selectively mutated the canonical DR5, upstream DR5 and upstream half-site and cloned these putative promoters into a promoterless luciferase reporter to generate four distinct reporter constructs. The canonical DR5 and upstream DR5 are the most important for the TTNPB response *in vivo* (Fig. 3A), whereas mutating the upstream half-site does not affect TTNPB responsiveness (Fig. 3A). Next, we designed both wild-type and mutated oligonucleotide pairs containing each RARE with 5 bp flanking sequence. RAR α , RAR β and RAR γ are all capable of binding the upstream and canonical RAREs as heterodimers with *Xenopus* RXR α (Fig. S5).

Loss of RAR β 2 makes larger and fewer somites, and thwarts hypaxial muscle migration

As *Rar β 1* is not expressed in the early embryo, we focused our analysis on *Rar β 2* and targeted both homologs (L and S) for MO



knockdown (Table S1) (Karpinka et al., 2015). We designed morpholinos selective for *Rarβ2* and found that knockdown of S or L homeologs produces similar phenotypes on *Myod* expression; however, the L knockdown produced a subjectively stronger effect (Fig. S6). A combination of both MOs produced the strongest phenotypes; therefore, a mixture was used for subsequent experiments. Although *Rarβ2* is specifically expressed in the hatching gland, we detected no difference in time to hatching or in the rate of hatching between *Rarβ2* MO and control MO-injected embryos (data not shown).

Rarβ2 is expressed in mature trunk somites (Fig. 1) and RA is important for somite patterning (Moreno and Kintner, 2004; Janesick et al., 2014); therefore, we asked whether somite morphology in MO-injected embryos was disrupted. Analysis of the general muscle marker *Myod* at stage 40 revealed that somite number is reduced; somites appear thicker and migration of hypaxial muscle (red arrows) is abolished in bilaterally microinjected *Rarβ2* MO embryos (Fig. 4A-C). Notably, the characteristic chevron-shaped somites seen in control embryos are transformed into U-shaped or straight somites in *Rarβ2* MO embryos and some embryos show significant disorganization and blurring of somite boundaries (Fig. 4C). The same phenotype is observed at stage 45, indicating that loss of hypaxial migration is not simply a developmental delay. These tadpoles are also paralyzed (see Discussion). Unilaterally microinjected *Rarβ2* MO embryos show thicker, fewer and disorganized somites, and loss of hypaxial migration (Fig. 4D-G). Melanophore migration also fails to occur on the injected side (compare with Fig. 4D,E). Expression of *Tbx3*, which marks hypaxial myoblasts (Martin et al., 2007), is knocked down and cells expressing *Tbx3* fail to migrate ventrally from the anterior trunk somites compared with the uninjected side (compare with Fig. 4F,G).

Unilateral knockdown of RARβ2 produces similar phenotypes to *Myod* expression at tailbud stage 26 (Fig. 5A,B). The thicker,

U-shaped morphology is predominant (Fig. 5B,C) but we also observed forked hypaxial regions (Fig. 5D), blurred somite domains (Fig. 5E) and criss-crossed somites (Fig. 5F), especially in the more anterior somites where *Rarβ2* is strongly expressed. Coronal sections were used to measure somite size and number (Fig. 5G,H). We observed a reduced number of somites on the injected side of *Rarβ2* MO embryos, and also a slight reduction in somite number on the uninjected side of *Rarβ2* MO embryos compared with control MO (Fig. 5I). We did not detect significant changes in the unsegmented PSM length (Fig. S7); however, deciphering the exact rostral PSM boundary from *Myod* expression and morphology alone is challenging. Increased somite length (Fig. 5J) was visible and significant in *Rarβ2* MO embryos, and is likely a strong contributing factor to decreased somite number, as more PSM cells are incorporated into each somite. We conclude that loss of *Rarβ2* yields fewer and bigger, U-shaped somites with impaired boundary formation.

Segmented PSM markers *Ripply2* and *Mespa/Thyl2* are most readily viewed at neurula stages where microinjection of *Rarβ2* MO shifts expression of these markers rostrally and each domain appears thicker (Fig. 6A,B) compared with control MO (Fig. S8A,B). The segmented boundaries of *Ripply2* are mostly maintained compared with *Rarγ*-MO embryos where *Ripply2* boundaries are lost (Janesick et al., 2014). Others have previously demonstrated that RA regulates laterality and coordinates left-right timing of the somitogenesis clock such that somites develop symmetrically across the midline (Kawakami et al., 2005; Vermot and Pourquié, 2005). Bilaterally injected *Rarβ2* MO embryos exhibited noticeable left-right asymmetry in 32% of the embryos (Fig. S9). Unsegmented PSM markers *Tbx6*, *Msn1*, *Fgf8* and *Esr5* are also shifted rostrally by *Rarβ2* MO (Fig. 6C-F) compared with control MO (Fig. S8C-F), a phenotype distinct from *Rarγ*-MO embryos where PSM and caudal expression is diminished (Janesick et al., 2014). Double

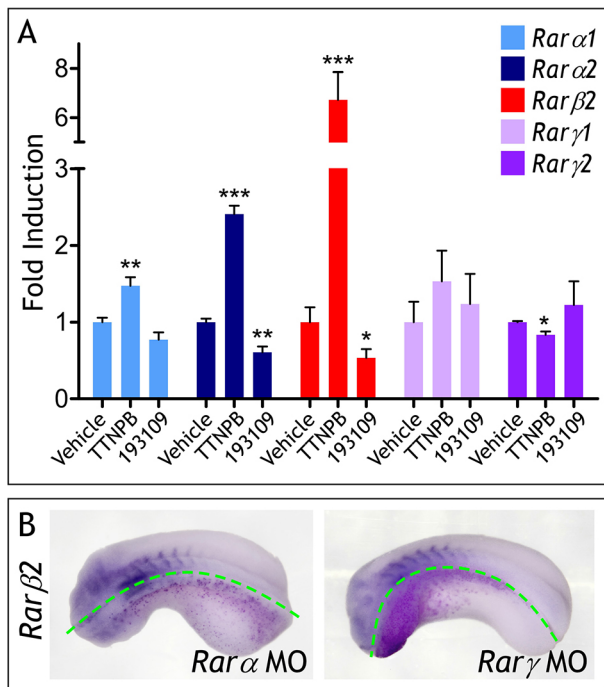


Fig. 2. *Rarβ2* is induced by TTNPB and is regulated by *RARα* and/or *RARγ*. (A) QPCR showing *Rarα1*, *Rarα2*, *Rarβ2*, *Rarγ1* and *Rarγ2* expression in embryos treated at stage 7/8 with 1 μM TTNPB, 1 μM AGN193109 or vehicle (0.1% ethanol) and collected at tailbud stage. The y-axis represents 2^{-ΔΔCt} values normalized to *Eef1a1* and expressed as fold induction relative to control vehicle ($n=5$ biological replicates) using standard propagation of error (Bevington and Robinson, 2003). Error bars indicate s.e.m. An unpaired *t*-test in GraphPad Prism v5.0 is reported (* $P \leq 0.05$, ** $P \leq 0.01$, *** $P \leq 0.001$). (B) Embryos were injected unilaterally at the 2- or 4-cell stage with 6.6 ng *Rarα* MOs or *Rarγ* MOs. The injected side is indicated by magenta β -gal lineage tracer. *Rarα* MOs and *Rarγ* MOs knock down the expression of *Rarβ2* (α MOs, 13/13 embryos; γ MOs, 8/8) at tailbud stage. Embryos are shown in dorsal view with anterior on the left. Midline is indicated by a broken green line.

whole-mount *in situ* hybridization analysis verified that *Rarβ2* and *Ripply2* expression do not overlap (Fig. S10) and presumably this is the case for other PSM markers that are equal or posterior to *Ripply2*

(Hitachi et al., 2008). This suggests that *RARβ2* is the receptor subtype that responds to RA and places *Rarβ2* in the correct position to confine expression of PSM and caudal progenitor genes to the posterior territory.

Ripply2 regulates somitogenesis downstream of RA via Groucho and Tbx6

Loss of somite chevron morphology is often attributed to deformities in the horizontal myoseptum and notochord (Rost et al., 2014). The myoseptum separates dorsal and ventral somite domains, and is required for aquatic locomotion. In zebrafish, the notochord is required for adaxial ‘muscle pioneers’, for myoseptum and for chevron somite morphology (Halpern et al., 1993; Brennan et al., 2002). We tested whether *Rarβ2* MO embryos possessed a normal notochord histologically and by looking at expression of *Xnot*. *Rarβ2* MO embryos form a notochord (not shown) and express *Xnot*, albeit the axis is shorter and crooked (Fig. S11B) compared with controls (Fig. S11A). Next, we investigated the expression of presumptive myoseptum or muscle pioneer markers, such as *Cxcl12*, *Notum*, *Netrin*, *Wnt11* and *Engrailed 1*, that have been established in zebrafish. Most markers tested by us, or viewed in Xenbase (Karpinka et al., 2015) are not specific to the myoseptum or adaxial pioneers but rather are: (1) not expressed, (2) expressed in the neural tube floor plate or interneurons, or (3) expressed within the entire somite domain (Fig. S12). Therefore, either *Xenopus* does not possess a marker for these cells/structures, or the myotome is not compartmentalized as in zebrafish (see Discussion).

Despite the lack of molecular markers for the myoseptum and adaxial cells, *Xenopus* still possesses chevron-shaped somites, which become U-shaped and disorganized in *Rarβ2* MO embryos. We hypothesized that the boundary-setting gene *Ripply2* is involved in the phenotype. *Ripply1/2* are spatially regulated by retinoids (Janesick et al., 2014; Moreno et al., 2008) and *Rarβ2* MO causes rostral expansion and broadened domains of *Ripply2* (Fig. 6A). We and others showed that developing organisms are exquisitely sensitive to misexpression of *Ripply* genes (Janesick et al., 2012; Li et al., 2013; Kawamura et al., 2005). *Ripply1* overexpression eliminates notochord and myoseptum (Kawamura et al., 2005) and

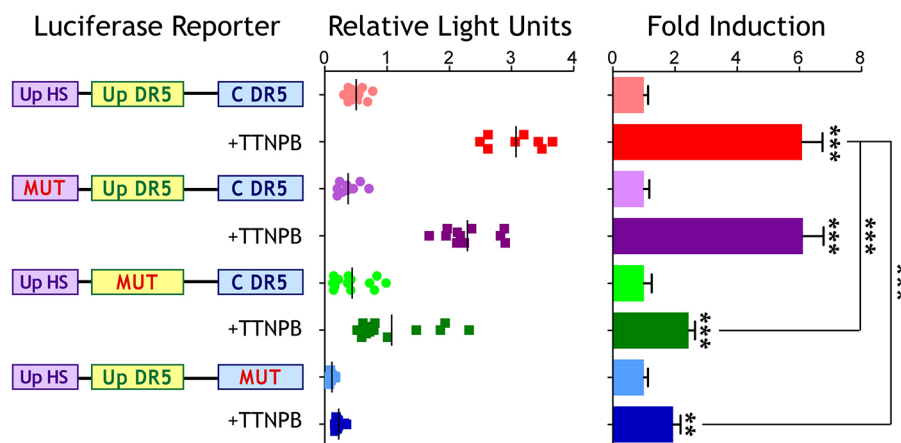


Fig. 3. *Xenopus laevis* *RARβ2* promoter elements are required for RA responsiveness. Luciferase reporters were selectively mutated for the canonical (C) direct repeat 5 (DR5) (Sucov et al., 1990), upstream DR5 and upstream half-site (HS). Embryos were injected unilaterally at the 2- or 4-cell stage with 50 pg reporter DNA then treated at blastula stage with 0.1 μM TTNPB or vehicle (0.1% ethanol). Embryos were collected at neurula stage (each data point represents one pool of 10 embryos). Data are represented either as relative light units measured by the luminometer or fold induction relative to vehicle using standard propagation of error (Bevington and Robinson, 2003). TTNPB responsiveness is reduced by mutating either the canonical DR5 or upstream DR5. Both basal reporter activity and TTNPB responsiveness is reduced by mutating the upstream half-site; however, fold induction is equivalent to wild type. Error bars indicate s.e.m. An unpaired *t*-test in GraphPad Prism v5.0 is reported (*** $P \leq 0.001$; ** $P \leq 0.01$).

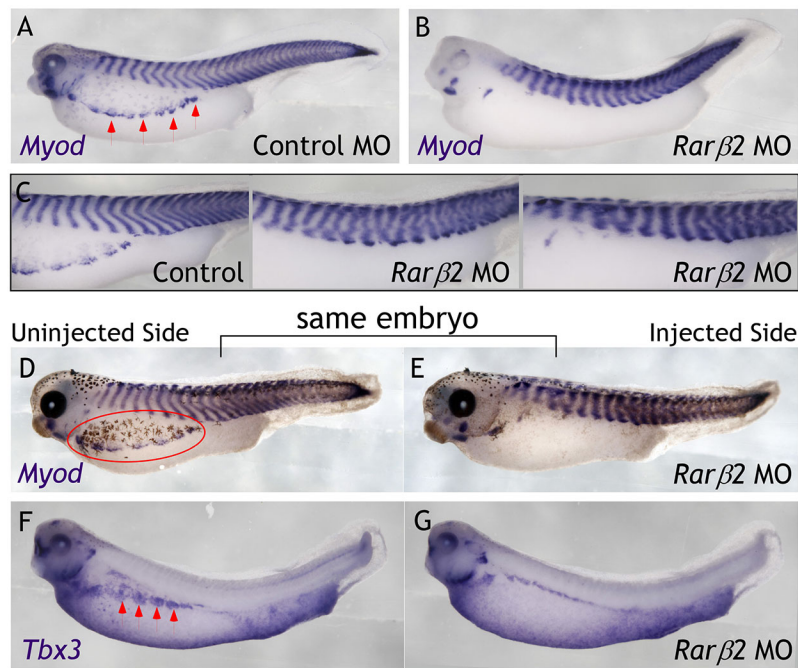


Fig. 4. Somite morphology and migration of hypaxial muscle migration are disrupted in *Rarβ2* MO-injected tadpoles. (A-C) Embryos were microinjected bilaterally at the 2-cell stage with 26 ng *Rarβ2.L*+26 ng *Rarβ2.S* MOs or 52 ng control MO. (A,B) *Rarβ2* MOs result in paralysis and curved body axis. *Myod* marks the somites that are thicker and fewer in number without v-shape morphology (17/18 embryos) compared with control MO. Red arrowheads indicate migrating hypaxial myoblasts in controls, not observed in *Rarβ2* MO-embryos. (C) Higher magnification of blurred/disorganized somite morphologies observed in some embryos marked by *Myod* in control and *Rarβ2* MO-injected embryos. (D-G) Embryos were microinjected unilaterally at the 2- or 4-cell stage with 26 ng *Rarβ2.L*+26 ng *Rarβ2.S* MOs. (D,E) The injected side displays thicker disorganized somites (marked by *Myod*) without v-shape morphology (20/21 embryos), compared with the un.injected side. Red outline indicates melanophores and migrating hypaxial muscle that are absent on the injected side. (F,G) The injected side shows diminished hypaxial *Tbx3* expression (11/12 embryos), compared with the robust hypaxial migration on the un.injected side (red arrowheads). All embryos are shown in lateral view at stage 40; anterior on the left.

Ripply proteins commonly associate with T-BOX proteins, converting them to transcriptional repressors in the presence of Groucho (Hitachi et al., 2009; Janesick et al., 2012; Kawamura et al., 2005, 2008; Kondow et al., 2006, 2007; Windner et al., 2015). *Tbx6* interacts with Ripply1 in zebrafish (Kawamura et al., 2008) and inhibits adaxial *Myod* expression, suppressing notochord formation (Goering et al., 2003). *Tbx3* is a potential direct RAR target (Ballim et al., 2012) and is expressed in the notochord and hypaxial muscle (Takabatake et al., 2000; Martin et al., 2007). Thus, *Ripply2*, *Tbx3* and *Tbx6* are plausible candidates to regulate somite

chevron morphology, presomitic mesoderm and hypaxial muscle migration.

There are two *Ripply2* orthologs in *Xenopus* termed *Bowline* (Kondow et al., 2006) and *Ledgerline* (Chan et al., 2006), and two homeologs for each in *X. laevis* (Fig. S13A). *Xenopus Ripply1* has apparently been lost during evolution (Janesick et al., 2012). *Ledgerline* and *Bowline* are both expressed in a *Ripply2*-like pattern. Neither *Ledgerline* nor *Bowline* is expressed in mature somites, in contrast to zebrafish *rippy1* (Kawamura et al., 2005). Notochord, which is marked by *Xnot* expression, is completely obliterated in

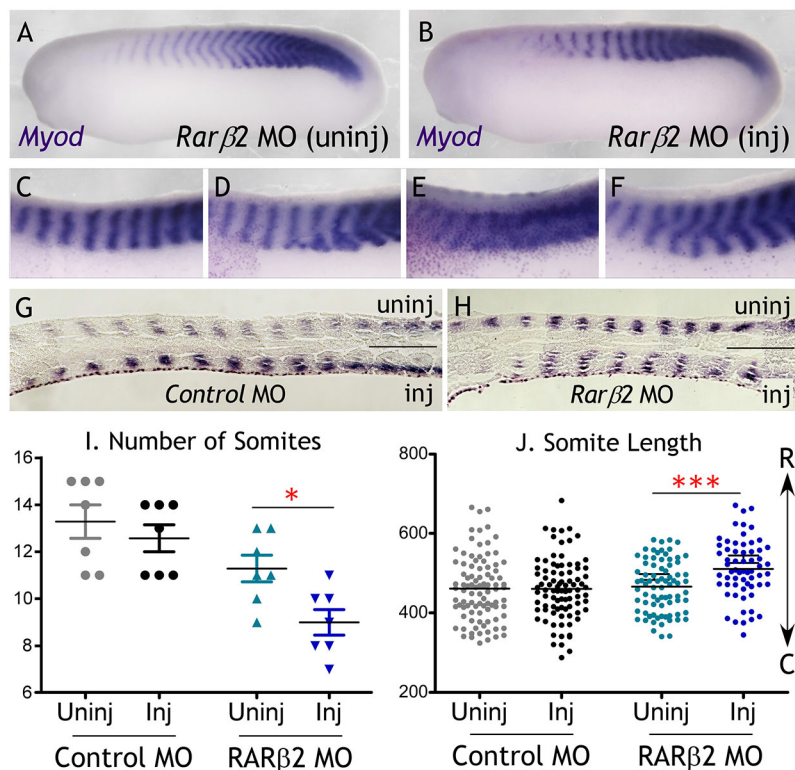


Fig. 5. Somite number is reduced and length increased in *Rarβ2* MO-injected embryos. (A-F) Embryos were microinjected unilaterally at the 2- or 4-cell stage with 26 ng *Rarβ2.L*+26 ng *Rarβ2.S* MOs or 52 ng control MO. (A,B) Two lateral sides of the same embryo are shown at stage 26; anterior on the left. Injected side is indicated by magenta β -gal lineage tracer. *Rarβ2* MOs (B) disrupt and disorganize the chevron-shaped somite morphology, reduce somite number and increase somite thickness (18/18 embryos) compared with the uninjected side (A), as indicated by *Myod* expression. (C-F) Higher magnification of somite morphologies (marked by *Myod*) on the *Rarβ2* MO-injected side observed in different embryos. (G,H) Paraffin wax-embedded coronal sections of embryos from (A-F). (I) Somite number is quantitated from sectioned embryos; each data point represents one embryo ($n=7$). (J) Somite size (length from posterior to anterior end) is quantitated from sectioned embryos using ImageJ (units are distance in pixels); each data point represents one somite. R, rostral somites; C, caudal somites. Statistics for I, J were calculated in GraphPad Prism v5 using a t-test (* $P \leq 0.05$; *** $P \leq 0.001$).

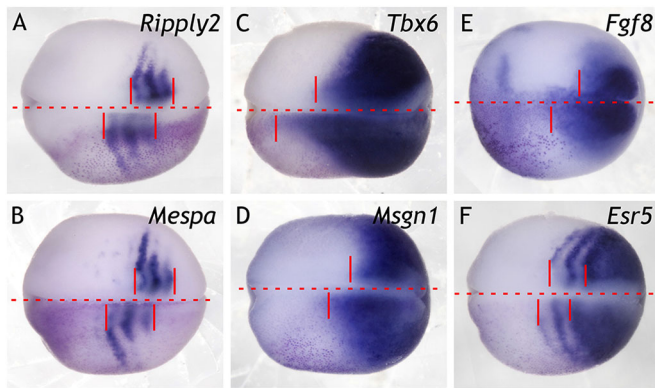


Fig. 6. Rostral shifting and expansion of somitomere and presomitic mesoderm markers occurs in *Rarβ2* MO-injected embryos. (A-F) Embryos were injected unilaterally at the 2- or 4-cell stage with 26 ng *Rarβ2.L* MO+26 ng *Rarβ2.S* MO. Injected side is indicated by magenta β -gal lineage tracer. Neurula stage embryos shown in dorsal view with anterior on the left. *Rarβ2* MOs rostrally shift somitomere markers *Ripply2* (A) and *Mespa/Thyl2* (B), and thicken their boundaries of expression (*Ripply2*, 25/27 embryos; *Mespa*, 26/31). The expression domains of presomitic mesoderm markers *Tbx6* (C), *Msgn1* (D) and *Fgf8* (E), and the Notch direct target *Esr5* (F) are expanded rostrally (red vertical lines) by *Rarβ2* MOs (*Tbx6*, 26/28 embryos; *Msgn1*, 7/9; *Fgf8*, 9/13; *Esr5*, 19/20). Broken red line indicates the midline.

embryos microinjected with *Bowline*, and hyperdorsalization or double axes are induced (Fig. S11C), a phenomenon we and others observed for *Ripply3* (Li et al., 2013). Embryos microinjected with *Ledgerline* diminished *Xnot* expression, but exhibited stronger axial defects (Fig. S11D). In embryos that still had body axes, we observed that *Myod* expression is completely abolished on the injected side (Fig. S13D).

Ripply2 has two conserved regions found in all *Ripply* family genes: a WRPW motif that facilitates interaction with Groucho (Fisher et al., 1996; Kondow et al., 2006) and an FPVQ motif that is predicted to mediate contacts with T-BOX proteins (Kawamura et al., 2008). We found that overexpression of *Ripply2* double mutants (WRPW→AAAA; FPVQ→AAAA), which presumably

cannot interact with Tbx or Groucho, are phenotypically normal in somite morphology, marked by *Myod* (Fig. S13D). Single-domain mutants (WRPW or FPVQ) are mostly normal except that *Ledgerline* WRPW mutants display an intermediate phenotype between wild type and double mutant overexpression (data not shown).

We have previously shown that *Ripply3* inhibits Tbx1 transcriptional activity *in vivo* (Janesick et al., 2012). Similarly, zebrafish *Ripply1* converts Tbx6 from a transcriptional activator to a repressor *in vitro* (Kawamura et al., 2008) and this protein interaction is essential for establishing the posterior somite boundary (Morimoto et al., 2007; Takahashi et al., 2010). We hypothesized that *Xenopus* *Ripply2* would also convert Tbx6 into a transcriptional repressor. Microinjection experiments showed that Tbx6 is a transcriptional activator (Fig. 7). *Xenopus* *Ripply2* (*Bowline* or *Ledgerline*) inhibits Tbx6 transcriptional activation *in vivo*, and this effect is blocked by mutation of the WRPW and FPVQ domains of *Ripply2* (Fig. 7). By contrast, Tbx3 is a transcriptional repressor *in vivo* (Fig. 7), substantiating previous *in vitro* reports (He et al., 1999; Hoogaars et al., 2004). Competition with mutant *Ripply2* mRNAs does not affect Tbx3 activity (Fig. 7); therefore, Tbx3 is unlikely to employ *Ripply2* as a co-repressor. We conclude that *Ripply2* is a retinoid-responsive gene modulating *Tbx6* activity in the presomitic mesoderm, but not *Tbx3* in the notochord and hypaxial muscle.

DISCUSSION

Characterization of *RARβ2*

Rarβ2 is the predominant *Rarβ* isoform in *X. laevis*. Both *Rara* and *Rarγ* are expressed earlier in developmental time and are required for the expression of *Rarβ2*. This is compatible with the observation that *Rarβ2* expression is lost in chicken embryos injected *in ovo* with antisense oligonucleotides blocking *Raraα2* (Cui et al., 2003). *RARβ2* expression is RA-regulated: deletion of 24 bp of the *Rarβ2* promoter, including the canonical RARE but sparing the TATA-box, abolished responsiveness to RA (Sucov et al., 1990). We identified a second RARE and additional half-site upstream of the

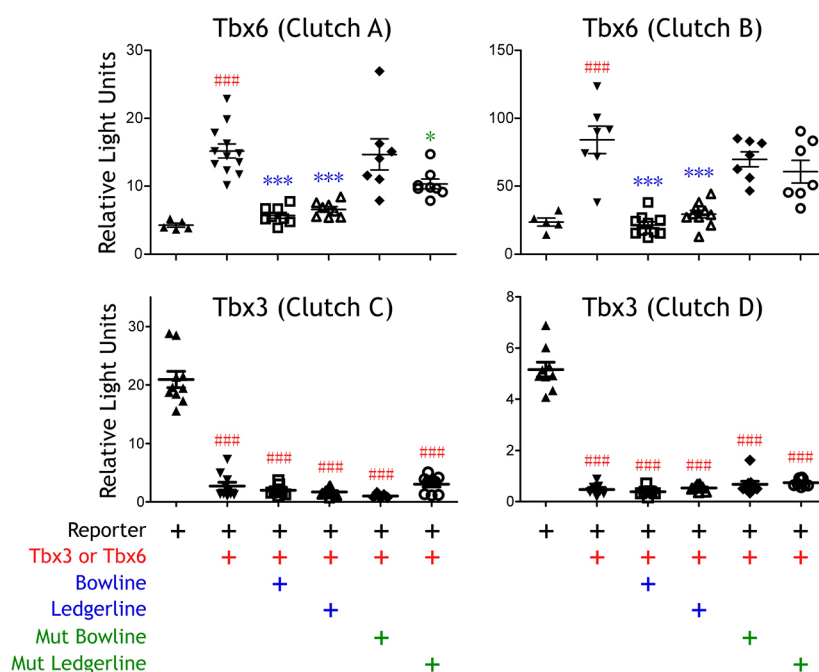


Fig. 7. *Tbx6* and *Tbx3* are differentially regulated by *Ripply2* *in vivo*. Whole-embryo luciferase assay reflecting Tbx6 or Tbx3 transcriptional activity in the presence or absence of wild-type or mutant *Ripply2* (*Bowline* or *Ledgerline*). Each data point represents one pool of five embryos, collected from different clutches of females (as indicated). Error bars indicate s.e.m. One-way ANOVA and Bonferroni's multiple comparison test was conducted using GraphPad Prism: ### $P \leq 0.001$ relative to reporter alone; *** $P \leq 0.001$ and * $P \leq 0.05$ relative to reporter+*Tbx6* mRNA. *Tbx6* increases activity ~3-fold. *Ripply2* (*Bowline* or *Ledgerline*) mRNAs repress activity to basal levels when co-injected with *Tbx6* mRNA; microinjection of *Ripply2* (*Bowline* or *Ledgerline*) mRNA mutated (Mut) for the WRPW and FPVQ domain does not repress *Tbx6* reporter activity. *Tbx3* reduces activity by about 90%, while *Ripply2* (*Bowline* or *Ledgerline* or mutants) does not affect *Tbx3* reporter activity.

canonical RAR β element, and showed that the second RARE also conferred activity in whole embryos. This second RARE might be redundant or could function as a shadow enhancer (Hong et al., 2008; Frankel et al., 2010; Perry et al., 2010) during different developmental times, or when vitamin A is less abundant. By contrast, we were unable to demonstrate activity in the conserved half-site. Although nuclear receptors can bind to half sites as monomers, this is not typically observed in RXR-dependent heterodimeric partners such as RAR (Mangelsdorf and Evans, 1995).

Our finding that *Rarb2* is the RAR subtype most strongly upregulated in response to the pan-RAR agonist TTNPB shows that *Rarb2* expression is sensitive and responsive to RA levels in the embryo. *Rarb2* is expressed in mature somites in *X. laevis*, is positioned closest to the presumed ALDH1A2 source of RA (Haselbeck et al., 1999) and is likely to be a primary responder to ligand. Previous studies have shown that RA upregulated the expression of *Rarb2* in mouse P19 cells in the presence of cycloheximide (Dey et al., 1994) and expanded reporter expression in the limbs of *Rarb2* promoter-lacZ transgenic mouse embryos (Mendelsohn et al., 1991). *Rarb2* is significantly affected in VAD embryos (Cui et al., 2003), suggesting that transcription of *Rarb2* requires RA. By contrast, we showed that *Rary* is inhibited by RAR agonist TTNPB, consistent with its role as an unliganded repressor that is required to maintain the presomitic mesoderm (PSM) and promote axial elongation (Janesick et al., 2014). Our working model is that *Rarb2* is activated in the trunk by RA to regulate somitogenesis, whereas *Rary* is present in the tail where RA is absent, sustaining the population of cells that will contribute to somites.

RAR β loss of function expands PSM markers and disrupts somite boundaries

Somitogenesis is a process born out of the proliferation of caudal progenitors, typically marked by *Wnt3* and *Fgf8*, which contribute to the unsegmented PSM (marked by *Tbx6* and *Msn1*). Newly forming somitomers make up the segmented PSM (marked by *Ripply2* and *Mespa/Thyl2*), and are subsequently epithelialized to become mature somites, marked by *Myod* and *Rarb2*. Loss of RAR β leads to the expansion of *Tbx6*, *Msn1* and *Fgf8*, and corresponding rostral shifts and wider expression domains in *Ripply2* and *Mespa*. The rostral expansion and shift of the PSM and somitomers is anticipated considering that: (1) activation by RAR yields the opposite phenotype – caudal expansion of somitomers and diminished PSM (Janesick et al., 2014; Moreno and Kintner, 2004); and (2) *Rarb2* expression in mature somites is spatially positioned to restrict the PSM. Other evidence supporting our results include the phenotypes of *Raldh2*^{-/-} embryos (Cunningham et al., 2015) and RA antagonist-treated embryos (Janesick et al., 2014), where *Tbx6* expression is significantly expanded. Our results also reinforce the phenomenon of RAR-FGF mutual antagonism (Diez del Corral et al., 2003). Recently, murine RAR β was demonstrated to be recruited to the *Fgf8* RARE in the trunk where it functioned as a transcriptional repressor (Kumar et al., 2016). If this mechanism is conserved in *Xenopus*, then loss of RAR β would relieve repression on the *Fgf8* enhancer, and *Fgf8* expression would be expanded rostrally, which is what we observe.

We hypothesized that the boundary-setting gene *Ripply2* would play an important role downstream of RAR β to explain the disorganized and muddled somite boundaries in *Rarb2* MO embryos. *Ripply1* and *Ripply2* are spatially regulated by retinoids (Janesick et al., 2014; Moreno et al., 2008) and *Ripply1* mutants lack

both a notochord and myosepta (Kawamura et al., 2005), which could alter chevron morphology (Rost et al., 2014). The *Ripply1* gene is absent in *Xenopus* (Janesick et al., 2012), but *Ripply2* has been duplicated to generate two syntenic genes, *Bowline* and *Ledgerline*. We found some phenotypic differences when overexpressing *Xenopus Ripply2* mRNAs: *Ledgerline* mRNA was a stronger inducer of axial defects, whereas *Bowline* mRNA was more effective at inhibiting notochord formation as marked by *Xnot* expression.

The correlation of rostral expansion and shifting of the unsegmented and segmented PSM in *Rarb2* MO embryos may be ascribed to their closely connected gene regulatory networks (reviewed by Dahmann et al., 2011). *Tbx6* induces expression of *Ripply1* (zebrafish) and *Ripply2* (*Xenopus*) (Windner et al., 2015; Hitachi et al., 2008). *Xenopus Tbx1* promotes expression of *Ripply3* in the pre-placodal ectoderm (Janesick et al., 2012), and murine *Tbx6* protein is responsible for setting the anterior boundary of *Mesp2* expression (Oginuma et al., 2008). Therefore, *Rarb2* MO-induced rostral expansion of *Tbx6* should alter somitome position in the same anteroposterior direction. The standard model is that *Tbx6* upregulates *Mespa*, setting the rostral somite border, which upregulates *Ripply1* and *Ripply2* to shut off *Tbx6* expression, thus setting the caudal border (reviewed by Dahmann et al., 2011). We wanted to know whether *Tbx6* transcriptional activity could be modulated by *Ripply2*. We found that *Ripply2* converts *Tbx6* to a transcriptional repressor, and that this is dependent on the WRPW (Groucho-interacting) and FPVQ (T-BOX interacting) domains of *Ripply2*. Hence, in areas where *Tbx6* and *Ripply2* are co-expressed, their interaction converts *Tbx6* into a transcriptional repressor that restricts its targets (presumably *Mespa*) and defines the posterior somitome boundary. RAR β loss of function results in the improper spatial positioning of *Tbx6*, *Mespa* and *Ripply2*, and widening of the *Mespa* and *Ripply2* domains, thus impairing this intricate regulatory pathway and disrupting somite boundaries.

RAR β loss of function reduces somite number and increases somite size

Anterior expansion of the PSM has been linked to the creation of smaller somites, which is attributable to increased proliferation, and a decreased number of cells differentiating into somites (Dubrulle et al., 2001; Hubaud and Pourquié, 2014). By a similar rationale, a larger PSM domain can cause somites to be displaced anteriorly, making fewer somites, as observed in *Shisa2*-MO embryos (Nagano et al., 2006). Although we observed reduced somite number in RAR β loss-of-function embryos, we found that the somites were larger, not smaller. We infer that the PSM is a limiting pool of cells; therefore, if more cells are being incorporated into each somite, then the final somite number will necessarily be reduced. One plausible explanation is that *Rarb2* MO extends or slows the segmentation clock period by modulating Notch signaling. Our previous microarray data have revealed that manipulation of RA signaling leads to significant changes in expression of oscillatory genes such as *Hes9.1*, *Hes3.3*, *Hes7.1*, *Hes5.2*, *Hey1* and *Hes2* (GEO Accession Number GSE57352). Increases in somite size have been observed in zebrafish and mouse, and are confusingly attributed to decreased and increased Notch signaling, respectively (reviewed by Oates et al., 2012). Notch-RAR crosstalk in somitogenesis has been poorly studied, although RA functions upstream of Notch signaling in primary neurogenesis (Franco et al., 1999). Importantly, as *Delta-1* is a direct target of *Tbx6* (White and Chapman, 2005), expansion of the *Tbx6* expression domain or protein levels could manipulate the speed of the clock. The current model in the field holds that there

is very tight coordination between the clock and wavefront position (reviewed by Wahi et al., 2016). Our data suggest that loss of RAR signaling might uncouple this connection. A future point of investigation will be to test whether manipulating Notch can rescue the *Rarβ2* MO somitogenesis phenotype. The possibility that RAR signaling could potentially control both the somitogenesis wavefront position and the timing of somite differentiation is intriguing and worthy of further investigation in the future.

RARβ2 is required for somite chevron morphology and hypaxial muscle migration

Although it was known that *Rarβ* is expressed in somites and lateral plate mesoderm (Cui et al., 2003; Ruberte et al., 1991; Romeih et al., 2003; Bayha et al., 2009), its role in somitogenesis was not addressed. A phenotype we observed with 100% penetrance in *Rarβ2* MO-injected embryos is the loss of chevron-shaped somite morphology, the appearance of thicker and fewer, U-shaped somites and inhibition of hypaxial muscle migration. The signature chevron somite shape is found in all aquatic creatures, and is indispensable for locomotion (Rost et al., 2014). RAR loss-of-function-induced paralysis in *Xenopus* was previously attributed to loss of primary neurons (Janesick et al., 2013; Sharpe and Goldstone, 1997; Blumberg et al., 1997). However, other factors that control locomotion (e.g. notochord integrity, neuromuscular junctions, central pattern generators, myotome differentiation and specialization) might also be contributing to movement defects in RAR mutants or RAR antagonist-treated embryos. The loss of chevron morphology in the somites may also contribute to the paralysis phenotype commonly observed with RAR loss of function.

In zebrafish, somite chevron morphology is attributed to the proper development of notochord and horizontal myoseptum that separates the hypaxial and epaxial myoblast lineages. Myosepta are laminar tendons that foster the attachment of notochord to somite muscle (Bassett and Currie, 2003) and are eventually populated by slow heavy chain fibers (Brent and Tabin, 2004). Myoseptum and adaxial/pioneer cells are not anatomy terms in *Xenopus* (Karpinka et al., 2015), and probes designed against genes that mark these structures in zebrafish did not mark them in *Xenopus*. The early compartmentalization of muscle in teleosts (fast versus slow, hypaxial/epaxial, adaxial/lateral) is not necessarily conserved in other vertebrates. Amniotes have a somitic architecture characterized as ‘peppered’ with respect to the physical locations of myotome subtypes (Brennan et al., 2002). Lampreys lack a myoseptum and adaxial cells (Hammond et al., 2009) despite possessing chevron-shaped somites (Rost et al., 2014). Differences in *Xenopus* and zebrafish have already been recognized with regard to somite rotation, intersomitic boundary formation and other early morphogenic movements in somitogenesis (Afonin et al., 2006; Henry et al., 2005; Leal et al., 2014). This could contribute to the difficulty in making direct comparisons between zebrafish and *Xenopus* with regard to myosepta, adaxial cells and chevron morphology.

In *Rarβ2* MO tadpole stage embryos, normal ventral migration of hypaxial myoblasts from the dermomyotome is inhibited. *Rarβ2* is undetectable in newly developing somitomers but predominantly expressed in the anteriormost 8-10 trunk somites, the same somites that contribute to hypaxial myoblast migration (Martin and Harland, 2001). Hypaxial delamination is RA dependent (Mic and Dueter, 2003), and our results suggest that RARβ2 is the receptor subtype modulating this process. We demonstrated that expression of *Tbx3*, a RAR direct target (Ballim et al., 2012) and hypaxial marker

(Martin et al., 2007), is diminished in RARβ2 morphants. *Tbx3* is normally found in discrete patches of cells, ventral to and separate from the somites in stage 40 tadpoles. *Rarβ2* loss of function disrupts this pattern, which was not attributable to developmental delay of migration.

In *Rarβ2* MO tadpole embryos, melanophore and hypaxial myoblast migration are inhibited, similar to the observation that *Pax3* ‘Splootch’ mutants lack both hypaxial muscle and melanocyte migration to the ventral belly (Auerbach, 1954; Brown et al., 2005). Melanophore and hypaxial migration are coordinated in *Xenopus* (Martin and Harland, 2001), although it has been proposed that melanophore and neural crest migration are not required for hypaxial migration (Martin and Harland, 2001). Both migrations are lost in RARβ2 loss of function, implying the existence of an upstream signal or developmental event connecting these processes. We conclude that *Rarβ2* is required for migration of hypaxial muscle, which could have implications for the proper patterning of hypaxial-derived structures, such as the rectus abdominus, limbs and tongue.

Loss of chevron morphology and hypaxial muscle was often accompanied by blurred somite boundaries and/or disordered somites; the epaxial and hypaxial domains, normally joined at the chevron apex, appeared to be disconnected from each other. An intriguing area for future study is how confusion of rostral/caudal polarity, caused by dysregulation of the *Ripply2/Tbx6/Mespa* transcriptional network early during somitogenesis, affects later development of epaxial/hypaxial muscle. This concept has been partly explored in zebrafish (Hollway et al., 2007). Our results suggest that the two processes are connected, because somite boundaries are disorganized and *Ripply2/Tbx6/Mespa* are misexpressed at early stages, whereas hypaxial myoblasts are absent (as marked by *Tbx3*) and somites continue to be disordered at later stages in RARβ2 loss of function embryos.

Conclusions

The requirement for retinoic acid signaling in somitogenesis is an established principle in developmental biology. Most attention has focused on how RA establishes the determination wavefront by

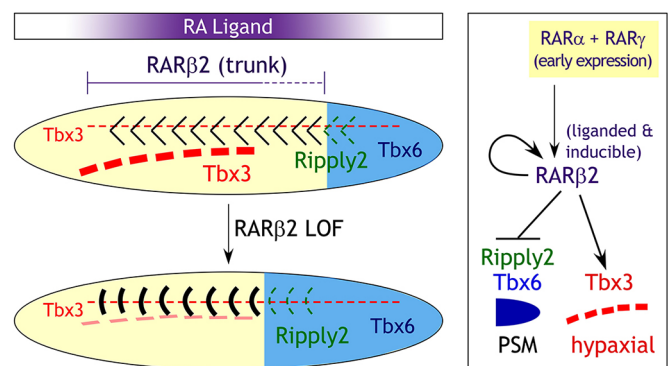


Fig. 8. Summary of RARβ2 loss-of-function phenotypes and RARβ2-mediated regulation of *Tbx6* and *Tbx3* in somitogenesis and hypaxial myoblast migration. *Xenopus Rarβ2* is the RAR subtype most upregulated in response to ligand. The localization of *Rarβ2* in the trunk somites positions it to respond to RA and control somitogenesis. RARβ2 regulates somite chevron morphology, restricts the PSM anterior boundary and promotes hypaxial myoblast migration. RARβ2 loss of function yields fewer and larger somites, often with disorganized or blurred domains. Ripply2 converts *Tbx6* to a transcriptional repressor *in vivo*, but does not influence *Tbx3* transcriptional activity. RARβ2 positively regulates *Tbx3* to promote hypaxial muscle migration and negatively regulates *Tbx6* to restrict the PSM and caudal progenitor pool.

antagonizing FGF and Wnt, restricting the PSM and caudal progenitor pool. Less was known about how RA regulates somite patterning or specification of myotome subdomains. Fig. 8 summarizes the findings in this paper. We show that *Rarβ2* is properly positioned to promote somitogenesis, and that it is the receptor subtype most likely to be responding to RA emanating from the trunk. The somitogenesis phenotype of RARβ2 loss of function is nuanced, but specific. In contrast to the RARγ loss of function phenotype, which reduces the PSM and the caudal progenitor pool, RARβ2 loss of function expands the PSM producing fewer and larger somites that lack chevron morphology and distinct boundaries. Migration of both melanophores and hypaxial myoblasts is completely inhibited in RARβ2 morphants. *Ripply2*, a recognized player in boundary setting, is rostrally shifted and broadened when RARβ2 is lost. *Ripply2* controls the transcriptional activity of *Tbx6* (PSM marker) but not *Tbx3* (hypaxial marker). Hence, RARβ2 positively regulates *Tbx3* to promote hypaxial muscle migration, but negatively regulates *Tbx6* to restrict the PSM.

MATERIALS AND METHODS

Embryo microinjection and whole-mount *in situ* hybridization

All experiments were approved by UC-Irvine IACUC. *Xenopus* eggs were fertilized *in vitro* and embryos staged as described previously (Janesick et al., 2012). Embryos were injected bilaterally or unilaterally at the two- or four-cell stage with gene-specific morpholinos (MO) (Table S1) and/or mRNA together with 100 pg/embryo β-galactosidase (β-gal) mRNA lineage tracer (LT). Embryos were maintained in 0.1× MBS until controls reached appropriate stages. Embryos processed for whole-mount *in situ* hybridization were fixed in MEMFA, stained with magenta-GAL (Biosynth) and stored in 100% ethanol (Janesick et al., 2012).

Whole-mount *in situ* hybridization was performed as previously described (Janesick et al., 2012). *Rarβ1*, *Rarβ2* (Session et al., 2016), *Xa-1* (Hemmati-Brivanlou et al., 1990), *Ripply2/Bowline* (Kondow et al., 2006), *Mespa* (Sparrow et al., 1998), *Mesogenin1* (Joseph and Cassetta, 1999), *Tbx3* (Li et al., 1997), *Tbx6* (Uchiyama et al., 2001), *Esr5* (Jen et al., 1999), *Myod* (Hopwood et al., 1989), *Cxcl12a* (Braun et al., 2002), *En1* (Watanabe et al., 1993) and *Myhpc1* (Session et al., 2016) probes were prepared via PCR amplification of coding regions incorporating a 3' bacteriophage T7 promoter. pCS2-*Fgf8* (a gift from Nancy Papalopulu) was linearized with *Bam*HI. Relevant primers and restriction enzymes are listed in Table S2. Probes were transcribed with MEGAscript T7 (Life Technologies) and digoxigenin-11-UTP (Roche). Embryos stained with *Myod* by whole-mount *in situ* hybridization were cleared in HistoClear and embedded in Paraplast+ using Sakura Finetek disposable base molds (15 mm×15 mm×5 mm) and yellow embedding rings. Serial coronal sections (8 μm) were mounted onto Superfrost+ microscope slides, dried overnight, dewaxed with xylene and photographed under bright-field illumination.

Embryo treatments and RT-QPCR

Microinjected embryos were treated at stage 7/8 with TTNPB (a RAR agonist), AGN193109 (a RAR-selective antagonist) or 0.1% ethanol (vehicle) in 0.1× MBS as described previously (Janesick et al., 2012) and aged until control embryos reached tailbud stage. Embryos from each treatment were randomly separated into groups of five embryos (each group of five embryos was taken as one biological replicate, *n*=1) and homogenized in 200 μl TriPure (Roche). Total RNA was DNase treated, LiCl precipitated, reverse transcribed into cDNA and quantitated in a Light Cycler 480 System (Roche) using the primer sets listed in Table S3 and SYBR green detection. Each primer set amplified a single band, as determined by gel electrophoresis and melting curve analysis. QPCR data for RAR staging were analyzed by ΔCt relative to *Histone H4* and corrected for amplification efficiency between RARs (Pfaffl, 2001). QPCR data for fold induction by RAR agonist and antagonist were analyzed using the ΔΔCt method relative to *Eef1a1*, normalizing to control embryos (Schmittgen and

Livak, 2008). Error bars represent biological replicates calculated using standard propagation of error (Bevington and Robinson, 2003).

Transient transfection and luciferase assays

pCDG1-*Tbx3*, pCDG1-*Tbx6* and pCDG1-*Ripply2* were constructed by PCR amplification of the *Xenopus laevis* *Tbx6* (Uchiyama et al., 2001), *Bowline* (Kondow et al., 2006) or *Ledgerline* (Chan et al., 2006) protein-coding regions. pCDG1-*Ripply2* mutant constructs were made by two-fragment PCR to generate the WRPW→AAAA and/or FPVQ→AAAA substitutions using the primers in Table S4. All constructs were cloned into the *Nco*I-*Bam*HI site of pCDG1, sequence verified and linearized with *Not*I. The 5'-capped mRNA was transcribed using T7 mMACHINE mMACHINE Kit (Thermo Fisher Scientific). pGL3-Basic-βRARE-Luciferase constructs were made by two-fragment PCR using primers in Table S5 and sequence verified. The (TBRE)₂-TK-luciferase reporter has been previously described (Janesick et al., 2012).

Embryos were microinjected unilaterally at the 2- or 4-cell stage with the βRARE-Luciferase reporter DNA, then treated as above at stage 7/8 with TTNPB or 0.1% ethanol (vehicle). When control embryos reached neurula stage, they were separated into groups of 10 embryos, homogenized and processed for luciferase assays as described previously (Janesick et al., 2014). Embryos were microinjected unilaterally at the 2- or 4-cell stage with the (TBRE)₂-TK-Luciferase reporter DNA, and different combinations of *Tbx3*, *Tbx6* and *Ripply2* (*Bowline* or *Ledgerline*) mRNA. When the embryos completed gastrulation, they were separated into groups of five embryos, homogenized and processed as described (Janesick et al., 2014).

Electrophoretic mobility shift assay

βRARE oligonucleotides (Table S6) were diluted in 1× buffer M (Roche) to 2.5 μM, heated to 95°C and annealed slowly. Free 5'-OH termini (10 pmol) was labeled with [γ-³²P] ATP (6000 Ci/mmol, 10 mCi/ml) using T4 PNK enzyme (Roche). Unincorporated label was removed using ProbeQuant G-50 microcolumns (Amersham Biosciences). RAR and RXR mRNA was synthesized using mMessage Machine T7 (Ambion) from *Not*I-linearized templates. Trace-labeled ³⁵S-Met-RAR and ³⁵S-Met-RXR protein was synthesized from RNA using Retic Lysate IVT Kit (Ambion). Binding of DNA and protein was performed as described previously (Umesono et al., 1991) and analyzed on 6%, non-denaturing polyacrylamide (29:1) gel, 0.5× TBE. Each gel was exposed overnight in a phosphorimaging cassette and visualized by phosphorimaging with a Typhoon PhosphorImager (GE HealthCare).

Acknowledgements

We thank Kristin Ampig and Jingmin Zhou for technical assistance with paraffin wax sectioning and the cloning of *Bowline* and *Ledgerline* constructs.

Competing interests

The authors declare no competing or financial interests.

Author contributions

Conceptualization: A.J., B.B.; Methodology: A.J., B.B.; Validation: A.J., W.T., B.B.; Formal analysis: A.J., W.T., T.T.L.N., B.B.; Investigation: A.J., W.T., T.T.L.N., B.B.; Resources: B.B.; Writing - original draft: A.J.; Writing - review & editing: A.J., B.B.; Visualization: A.J., W.T., B.B.; Supervision: A.J., B.B.; Project administration: A.J., B.B.; Funding acquisition: B.B.

Funding

Supported by grants from the National Science Foundation (IOS-0719576 and IOS-1147236) to B.B.

Supplementary information

Supplementary information available online at <http://dev.biologists.org/lookup/doi/10.1242/dev.144345.supplemental>

References

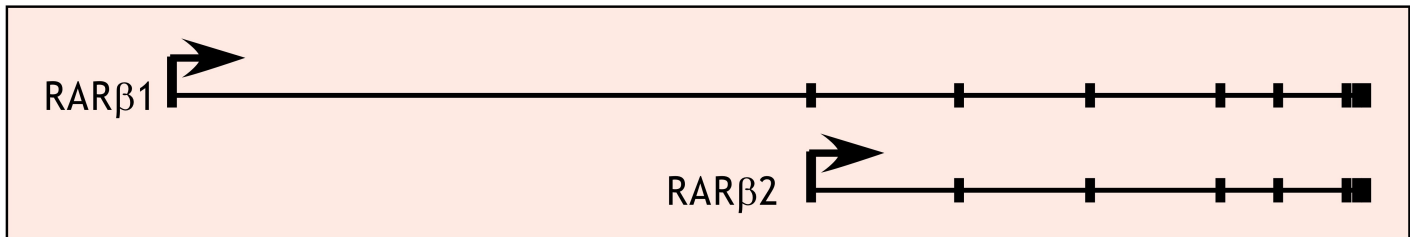
- Afonin, B., Ho, M., Gustin, J. K., Meloty-Kapella, C. and Domingo, C. R. (2006). Cell behaviors associated with somite segmentation and rotation in *Xenopus laevis*. *Dev. Dyn.* **235**, 3268-3279.
- Albalat, R., Brunet, F., Laudet, V. and Schubert, M. (2011). Evolution of retinoid and steroid signaling: vertebrate diversification from an amphioxus perspective. *Genome Biol. Evol.* **3**, 985-1005.

- Auerbach, R. (1954). Analysis of the developmental effects of a lethal mutation in the house mouse. *J. Exp. Zool.* **127**, 305-329.
- Ballim, R. D., Mendelsohn, C., Papaioannou, V. E. and Prince, S. (2012). The ulnar-mammary syndrome gene, *Tbx3*, is a direct target of the retinoic acid signaling pathway, which regulates its expression during mouse limb development. *Mol. Biol. Cell* **23**, 2362-2372.
- Bassett, D. I. and Currie, P. D. (2003). The zebrafish as a model for muscular dystrophy and congenital myopathy. *Hum. Mol. Genet.* **12** Suppl. 2, R265-R270.
- Bayha, E., Jørgensen, M. C., Serup, P. and Grapin-Botton, A. (2009). Retinoic acid signaling organizes endodermal organ specification along the entire antero-posterior axis. *PLoS ONE* **4**, e5845.
- Bevington, P. R. and Robinson, D. K. (2003). *Data Reduction and Error Analysis for the Physical Sciences*. New York City: McGraw-Hill Education.
- Blumberg, B., Bolado, J., Jr, Moreno, T. A., Kintner, C., Evans, R. M. and Papalopulu, N. (1997). An essential role for retinoid signaling in anteroposterior neural patterning. *Development* **124**, 373-379.
- Brand, N. J., Petkovich, M. and Chambon, P. (1990). Characterization of a functional promoter for the human retinoic acid receptor-alpha (hRAR-alpha). *Nucleic Acids Res.* **18**, 6799-6806.
- Braun, M., Wunderlin, M., Spieth, K., Knochel, W., Gierschik, P. and Moepps, B. (2002). Xenopus laevis Stromal cell-derived factor 1: conservation of structure and function during vertebrate development. *J. Immunol.* **168**, 2340-2347.
- Brennan, C., Amacher, S. L. and Currie, P. D. (2002). IV. Aspects of organogenesis: somitogenesis. In *Pattern Formation in Zebrafish* (ed. L. Solnica-Krezel), pp. 271-297. Berlin, Heidelberg: Springer.
- Brent, A. E. and Tabin, C. J. (2004). White meat or dark? *Nat. Genet.* **36**, 8-10.
- Brown, C. B., Engleka, K. A., Wenning, J., Min Lu, M. and Epstein, J. A. (2005). Identification of a hypaxial somite enhancer element regulating Pax3 expression in migrating myoblasts and characterization of hypaxial muscle Cre transgenic mice. *Genesis* **41**, 202-209.
- Chan, T., Satow, R., Kitagawa, H., Kato, S. and Asashima, M. (2006). Ledgerline, a novel Xenopus laevis gene, regulates differentiation of presomitic mesoderm during somitogenesis. *Zoolog. Sci.* **23**, 689-697.
- Cheng, L., Alvares, L. E., Ahmed, M. U., El-Hanfy, A. S. and Dietrich, S. (2004). The epaxial-hypaxial subdivision of the avian somite. *Dev. Biol.* **274**, 348-369.
- Chiang, M.-Y., Misner, D., Kempermann, G., Schikorski, T., Giguère, V., Sucov, H. M., Gage, F. H., Stevens, C. F. and Evans, R. M. (1998). An essential role for retinoid receptors RARbeta and RXRgamma in long-term potentiation and depression. *Neuron* **21**, 1353-1361.
- Cui, J., Michaille, J.-J., Jiang, W. and Zile, M. H. (2003). Retinoid receptors and vitamin A deficiency: differential patterns of transcription during early avian development and the rapid induction of RARs by retinoic acid. *Dev. Biol.* **260**, 496-511.
- Cunningham, T. J., Brade, T., Sandell, L. L., Lewandoski, M., Trainor, P. A., Colas, A., Mercola, M. and Duester, G. (2015). Retinoic acid activity in undifferentiated neural progenitors is sufficient to fulfill its role in restricting Fgf8 expression for somitogenesis. *PLoS ONE* **10**, e0137894.
- Dahmann, C., Oates, A. C. and Brand, M. (2011). Boundary formation and maintenance in tissue development. *Nat. Rev. Genet.* **12**, 43-55.
- D'aniello, E., Rydeen, A. B., Anderson, J. L., Mandal, A. and Waxman, J. S. (2013). Depletion of retinoic acid receptors initiates a novel positive feedback mechanism that promotes teratogenic increases in retinoic acid. *PLoS Genet.* **9**, e1003689.
- de The, H., del Mar Vivanco-Ruiz, M., Tiollais, P., Stunnenberg, H. and Dejean, A. (1990). Identification of a retinoic acid responsive element in the retinoic acid receptor beta gene. *Nature* **343**, 177-180.
- Dequéant, M. L. and Pourquié, O. (2008). Segmental patterning of the vertebrate embryonic axis. *Nat. Rev. Genet.* **9**, 370-382.
- Dey, A., Minucci, S. and Ozato, K. (1994). Ligand-dependent occupancy of the retinoic acid receptor beta 2 promoter in vivo. *Mol. Cell. Biol.* **14**, 8191-8201.
- Dietrich, S., Schubert, F. R., Healy, C., Sharpe, P. T. and Lumsden, A. (1998). Specification of the hypaxial musculature. *Development* **125**, 2235-2249.
- Diez Del Corral, R., Olivera-Martinez, I., Goriely, A., Gale, E., Maden, M. and Storey, K. (2003). Opposing FGF and retinoid pathways control ventral neural pattern, neuronal differentiation, and segmentation during body axis extension. *Neuron* **40**, 65-79.
- Dubrule, J., McGrew, M. J. and Pourquié, O. (2001). FGF signaling controls somite boundary position and regulates segmentation clock control of spatiotemporal Hox gene activation. *Cell* **106**, 219-232.
- Escriva, H., Bertrand, S., Germain, P., Robinson-Rechavi, M., Umbhauer, M., Cartry, J., Duffraisse, M., Holland, L., Gronemeyer, H. and Laudet, V. (2006). Neofunctionalization in vertebrates: the example of retinoic acid receptors. *PLoS Genet.* **2**, e102.
- Fisher, A. L., Ohsako, S. and Caudy, M. (1996). The WRPW motif of the hairy-related basic helix-loop-helix repressor proteins acts as a 4-amino-acid transcription repression and protein-protein interaction domain. *Mol. Cell. Biol.* **16**, 2670-2677.
- Franco, P. G., Paganelli, A. R., Lopez, S. L. and Carrasco, A. E. (1999). Functional association of retinoic acid and hedgehog signaling in Xenopus primary neurogenesis. *Development* **126**, 4257-4265.
- Frankel, N., Davis, G. K., Vargas, D., Wang, S., Payre, F. and Stern, D. L. (2010). Phenotypic robustness conferred by apparently redundant transcriptional enhancers. *Nature* **466**, 490-493.
- Garnaas, M. K., Cutting, C. C., Meyers, A., Kelsey, P. B., Jr, Harris, J. M., North, T. E. and Goessling, W. (2012). Rargb regulates organ laterality in a zebrafish model of right atrial isomerism. *Dev. Biol.* **372**, 178-189.
- Ghyselinck, N. B., Dupe, V., Dierich, A., Messaddeq, N., Garnier, J. M., Rochette-Egly, C., Chambon, P. and Mark, M. (1997). Role of the retinoic acid receptor beta (RARbeta) during mouse development. *Int. J. Dev. Biol.* **41**, 425-447.
- Goering, L. M., Hoshijima, K., Hug, B., Bisgrove, B., Kispert, A. and Grunwald, D. J. (2003). An interacting network of T-box genes directs gene expression and fate in the zebrafish mesoderm. *Proc. Natl. Acad. Sci. USA* **100**, 9410-9415.
- Hale, L. A., Tallafuss, A., Yan, Y.-L., Dudley, L., Eisen, J. S. and Postlethwait, J. H. (2006). Characterization of the retinoic acid receptor genes *raraa*, *rarab* and *rarg* during zebrafish development. *Gene Expr. Patterns* **6**, 546-555.
- Halpern, M. E., Ho, R. K., Walker, C. and Kimmel, C. B. (1993). Induction of muscle pioneers and floor plate is distinguished by the zebrafish no tail mutation. *Cell* **75**, 99-111.
- Hammond, K. L., Baxendale, S., Mccauley, D. W., Ingham, P. W. and Whitfield, T. T. (2009). Expression of patched, *prdm1* and engrailed in the lamprey somite reveals conserved responses to Hedgehog signaling. *Evol. Dev.* **11**, 27-40.
- Haselbeck, R. J., Hoffmann, I. and Duester, G. (1999). Distinct functions for *Aldh1* and *Raldh2* in the control of ligand production for embryonic retinoid signaling pathways. *Dev. Genet.* **25**, 353-364.
- He, M., Wen, L., Campbell, C. E., Wu, J. Y. and Rao, Y. (1999). Transcription repression by Xenopus ET and its human ortholog *TBX3*, a gene involved in ulnar-mammary syndrome. *Proc. Natl. Acad. Sci. USA* **96**, 10212-10217.
- He, X., Yan, Y.-L., Eberhart, J. K., Herpin, A., Wagner, T. U., Scharf, M. and Postlethwait, J. H. (2011). miR-196 regulates axial patterning and pectoral appendage initiation. *Dev. Biol.* **357**, 463-477.
- Hemmati-Brivanlou, A., Frank, D., Bolce, M. E., Brown, B. D., Sive, H. L. and Harland, R. M. (1990). Localization of specific mRNAs in Xenopus embryos by whole-mount in situ hybridization. *Development* **110**, 325-330.
- Henry, C. A., McNulty, I. M., Durst, W. A., Munchel, S. E. and Amacher, S. L. (2005). Interactions between muscle fibers and segment boundaries in zebrafish. *Dev. Biol.* **287**, 346-360.
- Hitachi, K., Kondow, A., Danno, H., Inui, M., Uchiyama, H. and Asashima, M. (2008). *Tbx6*, *Thylacine1*, and *E47* synergistically activate bowline expression in Xenopus somitogenesis. *Dev. Biol.* **313**, 816-828.
- Hitachi, K., Danno, H., Tazumi, S., Aihara, Y., Uchiyama, H., Okabayashi, K., Kondow, A. and Asashima, M. (2009). The Xenopus Bowline/Ripply family proteins negatively regulate the transcriptional activity of T-box transcription factors. *Int. J. Dev. Biol.* **53**, 631-639.
- Hollway, G. E., Bryson-Richardson, R. J., Berger, S., Cole, N. J., Hall, T. E. and Currie, P. D. (2007). Whole-somite rotation generates muscle progenitor cell compartments in the developing zebrafish embryo. *Dev. Cell* **12**, 207-219.
- Hong, J.-W., Hendrix, D. A. and Levine, M. S. (2008). Shadow enhancers as a source of evolutionary novelty. *Science* **321**, 1314.
- Hoogaars, W. M., Tessari, A., Moorman, A. F., de Boer, P. A., Hagoort, J., Soufan, A. T., Campione, M. and Christoffels, V. M. (2004). The transcriptional repressor *Tbx3* delineates the developing central conduction system of the heart. *Cardiovasc. Res.* **62**, 489-499.
- Hopwood, N. D., Pluck, A. and Gurdon, J. B. (1989). MyoD expression in the forming somites is an early response to mesoderm induction in Xenopus embryos. *EMBO J.* **8**, 3409-3417.
- Hubaud, A. and Pourquié, O. (2014). Signalling dynamics in vertebrate segmentation. *Nat. Rev. Mol. Cell Biol.* **15**, 709-721.
- Janesick, A., Shiotsugu, J., Taketani, M. and Blumberg, B. (2012). RIPPLY3 is a retinoic acid-inducible repressor required for setting the borders of the pre-placodal ectoderm. *Development* **139**, 1213-1224.
- Janesick, A., Abbey, R., Chung, C., Liu, S., Taketani, M. and Blumberg, B. (2013). ERF and ETV3L are retinoic acid-inducible repressors required for primary neurogenesis. *Development* **140**, 3095-3106.
- Janesick, A., Nguyen, T. T. L., Aisaki, K., Igarashi, K., Kitajima, S., Chandraratna, R. A. S., Kanno, J. and Blumberg, B. (2014). Active repression by RARGamma signaling is required for vertebrate axial elongation. *Development* **141**, 2260-2270.
- Jen, W.-C., Gawantka, V., Pollet, N., Niehrs, C. and Kintner, C. (1999). Periodic repression of Notch pathway genes governs the segmentation of Xenopus embryos. *Genes Dev.* **13**, 1486-1499.
- Joseph, E. M. and Cassetta, L. A. (1999). Mesp2: a novel basic helix-loop-helix gene expressed in the presomitic mesoderm and posterior tailbud of Xenopus embryos. *Mech. Dev.* **82**, 191-194.
- Karpinka, J. B., Fortriede, J. D., Burns, K. A., James-Zorn, C., Ponferrada, V. G., Lee, J., Karimi, K., Zorn, A. M. and Vize, P. D. (2015). Xenbase, the Xenopus model organism database; new virtualized system, data types and genomes. *Nucleic Acids Res.* **43** (Database issue), D756-D763.
- Kawakami, Y., Raya, A., Raya, R. M., Rodríguez-Esteban, C. and Izpisua Belmonte, J. C. (2005). Retinoic acid signalling links left-right asymmetric

- patterning and bilaterally symmetric somitogenesis in the zebrafish embryo. *Nature* **435**, 165-171.
- Kawamura, A., Koshida, S., Hijikata, H., Ohbayashi, A., Kondoh, H. and Takada, S.** (2005). Groucho-associated transcriptional repressor ripply1 is required for proper transition from the presomitic mesoderm to somites. *Dev. Cell* **9**, 735-744.
- Kawamura, A., Koshida, S. and Takada, S.** (2008). Activator-to-repressor conversion of T-box transcription factors by the Ripply family of Groucho/TLE-associated mediators. *Mol. Cell. Biol.* **28**, 3236-3244.
- Koide, T., Downes, M., Chandraratna, R. A., Blumberg, B. and Umesono, K.** (2001). Active repression of RAR signaling is required for head formation. *Genes Dev.* **15**, 2111-2121.
- Kondow, A., Hitachi, K., Ikegame, T. and Asashima, M.** (2006). Bowline, a novel protein localized to the presomitic mesoderm, interacts with Groucho/TLE in *Xenopus*. *Int. J. Dev. Biol.* **50**, 473-479.
- Kondow, A., Hitachi, K., Okabayashi, K., Hayashi, N. and Asashima, M.** (2007). Bowline mediates association of the transcriptional corepressor XGrg-4 with Tbx6 during somitogenesis in *Xenopus*. *Biochem. Biophys. Res. Commun.* **359**, 959-964.
- Kumar, S., Cunningham, T. J. and Duester, G.** (2016). Nuclear receptor corepressors Ncor1 and Ncor2 (Smrt) are required for retinoic acid-dependent repression of Fgf8 during somitogenesis. *Dev. Biol.* **418**, 204-15.
- Leal, M. A., Fickel, S. R., Sabillo, A., Ramirez, J., Vergara, H. M., Nave, C., Saw, D. and Domingo, C. R.** (2014). The Role of Sdf-1alpha signaling in *Xenopus laevis* somite morphogenesis. *Dev. Dyn.* **243**, 509-526.
- Leroy, P., Krust, A., Zelent, A., Mendelsohn, C., Garnier, J. M., Kastner, P., Dierich, A. and Chambon, P.** (1991). Multiple isoforms of the mouse retinoic acid receptor alpha are generated by alternative splicing and differential induction by retinoic acid. *EMBO J.* **10**, 59-69.
- Li, H., Tierney, C., Wen, L., Wu, J. Y. and Rao, Y.** (1997). A single morphogenetic field gives rise to two retina primordia under the influence of the prechordal plate. *Development* **124**, 603-615.
- Li, H.-Y., Grifone, R., Saquet, A., Carron, C. and Shi, D.-L.** (2013). The *Xenopus* homologue of Down syndrome critical region protein 6 drives dorsoanterior gene expression and embryonic axis formation by antagonising polycomb group proteins. *Development* **140**, 4903-4913.
- Linville, A., Radtke, K., Waxman, J. S., Yelon, D. and Schilling, T. F.** (2009). Combinatorial roles for zebrafish retinoic acid receptors in the hindbrain, limbs and pharyngeal arches. *Dev. Biol.* **325**, 60-70.
- Lohnes, D., Mark, M., Mendelsohn, C., Dolle, P., Dierich, A., Gorry, P., Gansmuller, A. and Chambon, P.** (1994). Function of the retinoic acid receptors (RARs) during development (I). Craniofacial and skeletal abnormalities in RAR double mutants. *Development* **120**, 2723-2748.
- Lufkin, T., Lohnes, D., Mark, M., Dierich, A., Gorry, P., Gaub, M. P., Lemeur, M. and Chambon, P.** (1993). High postnatal lethality and testis degeneration in retinoic acid receptor alpha mutant mice. *Proc. Natl. Acad. Sci. USA* **90**, 7225-7229.
- Maden, M.** (2007). Retinoic acid in the development, regeneration and maintenance of the nervous system. *Nat. Rev. Neurosci.* **8**, 755-765.
- Maden, M.** (2010). Analysis of retinoid signaling in embryos. In *Analysis of Growth Factor Signaling in Embryos* (ed. M. Whitman and A. Sater), pp. 87-128. Boca Raton, FL: CRC Press.
- Mangelsdorf, D. J. and Evans, R. M.** (1995). The RXR heterodimers and orphan receptors. *Cell* **83**, 841-850.
- Mark, M., Ghyselinck, N. B. and Chambon, P.** (2006). Function of retinoid nuclear receptors: lessons from genetic and pharmacological dissections of the retinoic acid signaling pathway during mouse embryogenesis. *Annu. Rev. Pharmacol. Toxicol.* **46**, 451-480.
- Martin, B. L. and Harland, R. M.** (2001). Hypaxial muscle migration during primary myogenesis in *Xenopus laevis*. *Dev. Biol.* **239**, 270-280.
- Martin, B. L., Peyrot, S. M. and Harland, R. M.** (2007). Hedgehog signaling regulates the amount of hypaxial muscle development during *Xenopus* myogenesis. *Dev. Biol.* **304**, 722-734.
- Massaro, G. D., Massaro, D., Chan, W. Y., Clerch, L. B., Ghyselinck, N., Chambon, P. and Chandraratna, R. A.** (2000). Retinoic acid receptor-beta: an endogenous inhibitor of the perinatal formation of pulmonary alveoli. *Physiol. Genomics* **4**, 51-57.
- Massaro, G. D., Massaro, D. and Chambon, P.** (2003). Retinoic acid receptor-alpha regulates pulmonary alveolus formation in mice after, but not during, perinatal period. *Am. J. Physiol. Lung Cell. Mol. Physiol.* **284**, L431-L433.
- Mendelsohn, C., Ruberte, E., Lemeur, M., Morriss-Kay, G. and Chambon, P.** (1991). Developmental analysis of the retinoic acid-inducible RAR-beta 2 promoter in transgenic animals. *Development* **113**, 723-734.
- Mic, F. A. and Duester, G.** (2003). Patterning of forelimb bud myogenic precursor cells requires retinoic acid signaling initiated by Raldh2. *Dev. Biol.* **264**, 191-201.
- Moreno, T. A. and Kintner, C.** (2004). Regulation of segmental patterning by retinoic acid signaling during *Xenopus* somitogenesis. *Dev. Cell* **6**, 205-218.
- Moreno, T. A., Jappelli, R., Izpisua Belmonte, J. C. and Kintner, C.** (2008). Retinoic acid regulation of the Mesp-Ripply feedback loop during vertebrate segmental patterning. *Dev. Biol.* **315**, 317-330.
- Morimoto, M., Sasaki, N., Oginuma, M., Kiso, M., Igarashi, K., Aizaki, K.-I., Kanno, J. and Saga, Y.** (2007). The negative regulation of Mesp2 by mouse Ripply2 is required to establish the rostro-caudal patterning within a somite. *Development* **134**, 1561-1569.
- Nagano, T., Takehara, S., Takahashi, M., Aizawa, S. and Yamamoto, A.** (2006). Shisa2 promotes the maturation of somitic precursors and transition to the segmental fate in *Xenopus* embryos. *Development* **133**, 4643-4654.
- Nakaya, Y., Kuroda, S., Katagiri, Y. T., Kaibuchi, K. and Takahashi, Y.** (2004). Mesenchymal-epithelial transition during somitic segmentation is regulated by differential roles of Cdc42 and Rac1. *Dev. Cell* **7**, 425-438.
- Niederreither, K. and Dollé, P.** (2008). Retinoic acid in development: towards an integrated view. *Nat. Rev. Genet.* **9**, 541-553.
- Nikaido, M., Kawakami, A., Sawada, A., Furutani-Seiki, M., Takeda, H. and Araki, K.** (2002). Tbx24, encoding a T-box protein, is mutated in the zebrafish somite-segmentation mutant fused somites. *Nat. Genet.* **31**, 195-199.
- Oates, A. C., Morelli, L. G. and Ares, S.** (2012). Patterning embryos with oscillations: structure, function and dynamics of the vertebrate segmentation clock. *Development* **139**, 625-639.
- Oginuma, M., Niwa, Y., Chapman, D. L. and Saga, Y.** (2008). Mesp2 and Tbx6 cooperatively create periodic patterns coupled with the clock machinery during mouse somitogenesis. *Development* **135**, 2555-2562.
- Perry, M. W., Boettiger, A. N., Bothma, J. P. and Levine, M.** (2010). Shadow enhancers foster robustness of *Drosophila* gastrulation. *Curr. Biol.* **20**, 1562-1567.
- Pfaffi, M. W.** (2001). A new mathematical model for relative quantification in real-time RT-PCR. *Nucleic Acids Res.* **29**, e45.
- Romeih, M., Cui, J., Michaille, J.-J., Jiang, W. and Zile, M. H.** (2003). Function of RARgamma and RARalpha2 at the initiation of retinoid signaling is essential for avian embryo survival and for distinct events in cardiac morphogenesis. *Dev. Dyn.* **228**, 697-708.
- Rost, F., Eugster, C., Schroter, C., Oates, A. C. and Brusch, L.** (2014). Chevron formation of the zebrafish muscle segments. *J. Exp. Biol.* **217**, 3870-3882.
- Ruberte, E., Dolle, P., Chambon, P. and Morriss-Kay, G.** (1991). Retinoic acid receptors and cellular retinoid binding proteins. II. Their differential pattern of transcription during early morphogenesis in mouse embryos. *Development* **111**, 45-60.
- Schmittgen, T. D. and Livak, K. J.** (2008). Analyzing real-time PCR data by the comparative C(T) method. *Nat. Protoc.* **3**, 1101-1108.
- Session, A., Uno, Y., Kwon, T., Chapman, J. A., Toyoda, A., Takahashi, S., Fukui, A., Hikosaka, A., Suzuki, A., Kondo, M. et al.** (2016). Genome evolution in the allotetraploid frog *Xenopus laevis*. *Nature* **538**, 336-343.
- Sharpe, C. R. and Goldstone, K.** (1997). Retinoid receptors promote primary neurogenesis in *Xenopus*. *Development* **124**, 515-523.
- Sparrow, D. B., Jen, W. C., Kotecha, S., Towers, N., Kintner, C. and Mohun, T. J.** (1998). Thylacine 1 is expressed segmentally within the paraxial mesoderm of the *Xenopus* embryo and interacts with the Notch pathway. *Development* **125**, 2041-2051.
- Srour, M., Chitayat, D., Caron, V., Chassaing, N., Bitoun, P., Patry, L., Cordier, M.-P., Capo-Chichi, J.-M., Francannet, C., Calvas, P. et al.** (2013). Recessive and dominant mutations in retinoic acid receptor beta in cases with microphthalmia and diaphragmatic hernia. *Am. J. Hum. Genet.* **93**, 765-772.
- Subbarayan, V., Kastner, P., Mark, M., Dierich, A., Gorry, P. and Chambon, P.** (1997). Limited specificity and large overlap of the functions of the mouse RAR gamma 1 and RAR gamma 2 isoforms. *Mech. Dev.* **66**, 131-142.
- Sucov, H. M., Murakami, K. K. and Evans, R. M.** (1990). Characterization of an autoregulated response element in the mouse retinoic acid receptor type beta gene. *Proc. Natl. Acad. Sci. USA* **87**, 5392-5396.
- Takabatake, Y., Takabatake, T. and Takeshima, K.** (2000). Conserved and divergent expression of T-box genes Tbx2-Tbx5 in *Xenopus*. *Mech. Dev.* **91**, 433-437.
- Takahashi, J., Ohbayashi, A., Oginuma, M., Saito, D., Mochizuki, A., Saga, Y. and Takada, S.** (2010). Analysis of Ripply1/2-deficient mouse embryos reveals a mechanism underlying the rostro-caudal patterning within a somite. *Dev. Biol.* **342**, 134-145.
- Takemoto, T., Uchikawa, M., Yoshida, M., Bell, D. M., Lovell-Badge, R., Papaioannou, V. E. and Kondoh, H.** (2011). Tbx6-dependent Sox2 regulation determines neural or mesodermal fate in axial stem cells. *Nature* **470**, 394-398.
- Uchiyama, H., Kobayashi, T., Yamashita, A., Ohno, S. and Yabe, S.** (2001). Cloning and characterization of the T-box gene Tbx6 in *Xenopus laevis*. *Dev. Growth Differ.* **43**, 657-669.
- Umesono, K., Murakami, K. K., Thompson, C. C. and Evans, R. M.** (1991). Direct repeats as selective response elements for the thyroid hormone, retinoic acid, and vitamin D3 receptors. *Cell* **65**, 1255-1266.
- Vermot, J. and Pourquié, O.** (2005). Retinoic acid coordinates somitogenesis and left-right patterning in vertebrate embryos. *Nature* **435**, 215-220.
- Wahi, K., Bochter, M. S. and Cole, S. E.** (2016). The many roles of Notch signaling during vertebrate somitogenesis. *Semin. Cell Dev. Biol.* **49**, 68-75.

- Watanabe, M., Hayashida, T., Nishimoto, T. and Kobayashi, H.** (1993). Nucleotide sequence of *Xenopus* homeobox gene, *En-1*. *Nucleic Acids Res.* **21**, 2513.
- Waxman, J. S. and Yelon, D.** (2007). Comparison of the expression patterns of newly identified zebrafish retinoic acid and retinoid X receptors. *Dev. Dyn.* **236**, 587-595.
- White, P. H. and Chapman, D. L.** (2005). *Dll1* is a downstream target of *Tbx6* in the paraxial mesoderm. *Genesis* **42**, 193-202.
- Windner, S. E., Doris, R. A., Ferguson, C. M., Nelson, A. C., Valentin, G., Tan, H., Oates, A. C., Wardle, F. C. and Devoto, S. H.** (2015). *Tbx6*, *Mesp-b* and *Ripply1* regulate the onset of skeletal myogenesis in zebrafish. *Development* **142**, 1159-1168.
- Zelent, A., Mendelsohn, C., Kastner, P., Krust, A., Garnier, J. M., Ruffenach, F., Leroy, P. and Chambon, P.** (1991). Differentially expressed isoforms of the mouse retinoic acid receptor beta generated by usage of two promoters and alternative splicing. *EMBO J.* **10**, 71-81.

A. Exon Structure



B. N-Terminal Variable Region

>XL_RARβ1.S (Chr. 6)

M**KT**SSRSC**SG**PAVN**GH**MNHYPASHYPFLFPPVIGGLSLPALHGLHGHPPTSGSSTPSPA**A**

>XL_RARβ1.L (Chr. 6)

M**MT**SSRSC**PV**PAVN**RH**MNHYPASHYPFLFPPVIGGLSLPALHGLHGHPPTSGSSTPSPA**T**

>XL_RARβ2.S; XL_RARβ2.L (Chr. 6)

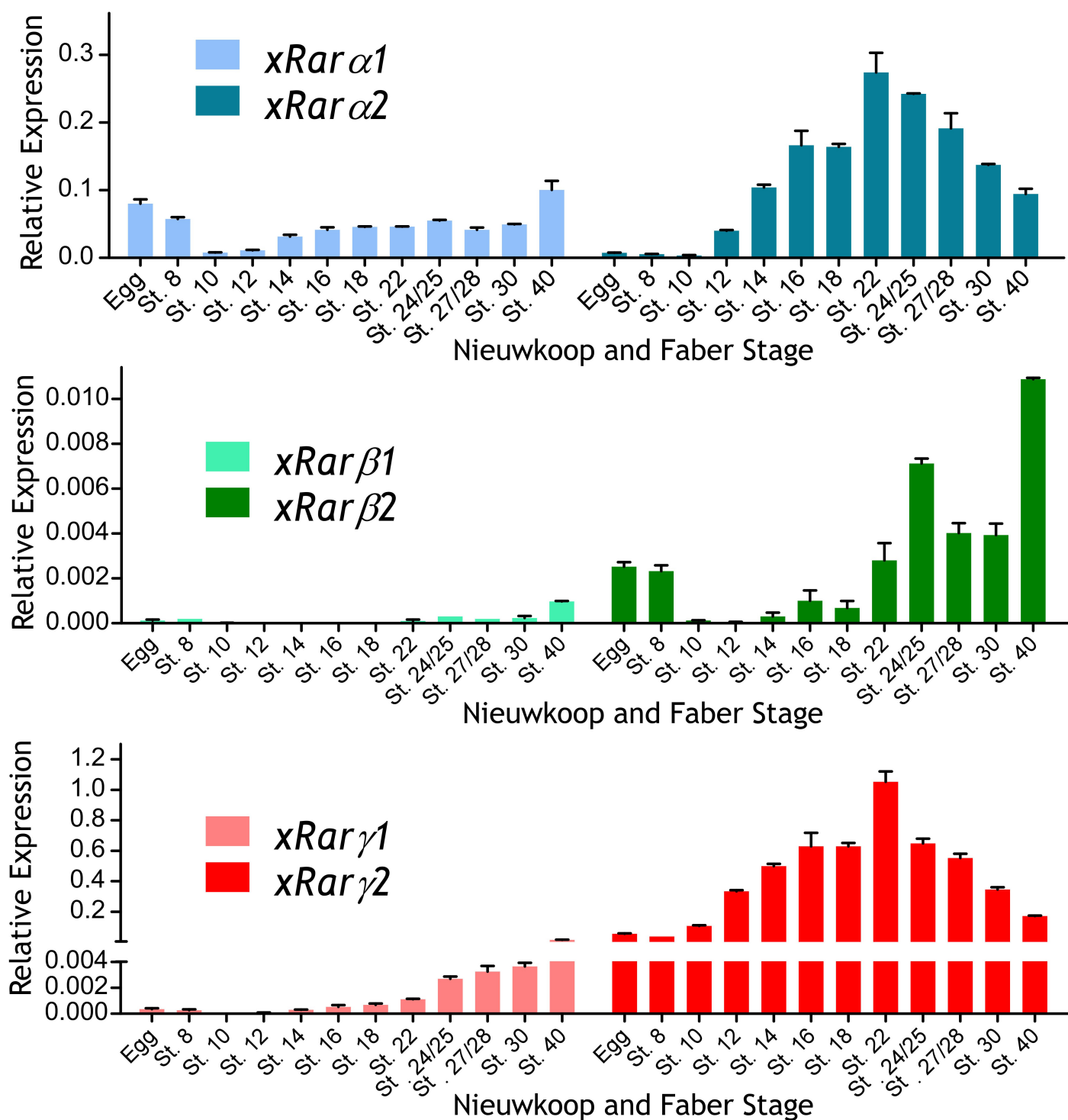
MFDCMDVLAVSPGQMLDFYTASPSSCMLQEKALKACFSGLAQTEWQHRHSAQS

C. Shared Region

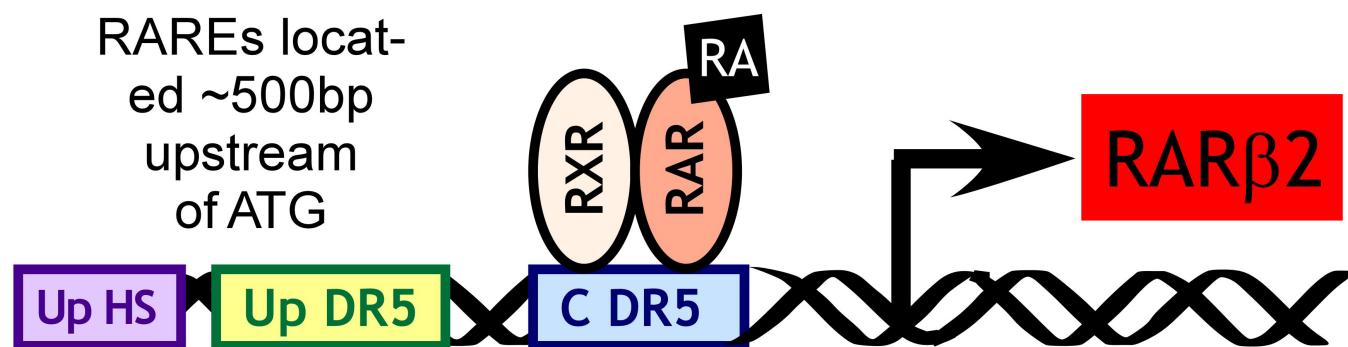
| | |
|--------------------|----------------------------------------------------------------------------------------------------------------------------------|
| XL_RARβ1/2.S_Ch. 6 | IETQSTSS ED LVPSPSPPPPPR VY KP CFVCQDKSSGYHYGVSACEGCKGFFRRSIQKNMVYTCHR |
| XL_RARβ1/2.L_Ch. 6 | IETQSTSS ED LVPSPSPPPPPR IY KP CFVCQDKSSGYHYGVSACEGCKGFFRRSIQKNMVYTCHR |
| XL_RARβ1/2.S_Ch. 6 | E KNCVINKVTRNRCQY CRLQRCFQ VGMSKESVRNDRNKKKKEPSK IEFTEN YEMTAELDDL AE KIR |
| XL_RARβ1/2.L_Ch. 6 | E KNCVINKVTRNRCQY CRLQRCFE VGMSKESVRNDRNKKKKEPSK QECIES YEMTAELDDL TE KIR |
| XL_RARβ1/2.S_Ch. 6 | KAHQ ET FP SLCQ LGKYTTN SSADQ RVRDLGLWDFSELATKCI IKIVEFAKRLPGFTSLTIADQI |
| XL_RARβ1/2.L_Ch. 6 | KAHQ ET FP SLCQ LGKYTTN SSADH RVRDLGLWDFSELATKCI IKIVEFAKRLPGFTSLTIADQI |
| XL_RARβ1/2.S_Ch. 6 | TLLKAA CLD LILIRICTRFTPEQDTMTFSDGLTLNRTQ MHNAGFGPLTDLVFTFANQLLPLEMDDT |
| XL_RARβ1/2.L_Ch. 6 | TLLKAA CLD LILIRICTRFTPEQDTMTFSDGLTLNRTQ MHNAGFGPLTDLVFTFANQLLPLEMDDT |
| XL_RARβ1/2.S_Ch. 6 | ETGLLSAICLIC ED RQDLEEP AKVDKLQ EPLLEALKIYIRKRRPNKPHMFPKI LMKITDLRSISAK |
| XL_RARβ1/2.L_Ch. 6 | ETGLLSAICLIC VD RQDLEEP AKVDKLQ EPLLEALKIYIRKRRPNKPHMFPKI LMKITDLRSISAK |
| XL_RARβ1/2.S_Ch. 6 | GA ERVITL KLEI PGSMPLIQEML ENSEGHE ASAA AS PTEDT KEHSHR ISPSS- EEEE R VSKCAR VQ |
| XL_RARβ1/2.L_Ch. 6 | GT ERVITL KLEI PGSMPLIQEML ENSEGLE ASAA PS PTEDT TEHSHC ISPSS EEEE H VSKCAQ VQ |

■ DNA Binding ■ Ligand Binding

Supplemental Figure S1. Exon structure and protein coding sequence of *Xenopus laevis* RARβ1.S, RARβ1.L, RARβ2.S, and RARβ2.L. Homeologs of RARβ, located on chromosome 6, are denoted by .L and .S notation. (A, B) RARβ1 and RARβ2 possess alternative promoters which alter the N-terminal region of the protein (bolded green residues = amino acids not conserved between homeologs). (C) Shared region of RARβ1 and RARβ2, with DNA binding domain in red, and ligand binding domain in blue. Bolded amino acid residues are not conserved between homeologs.



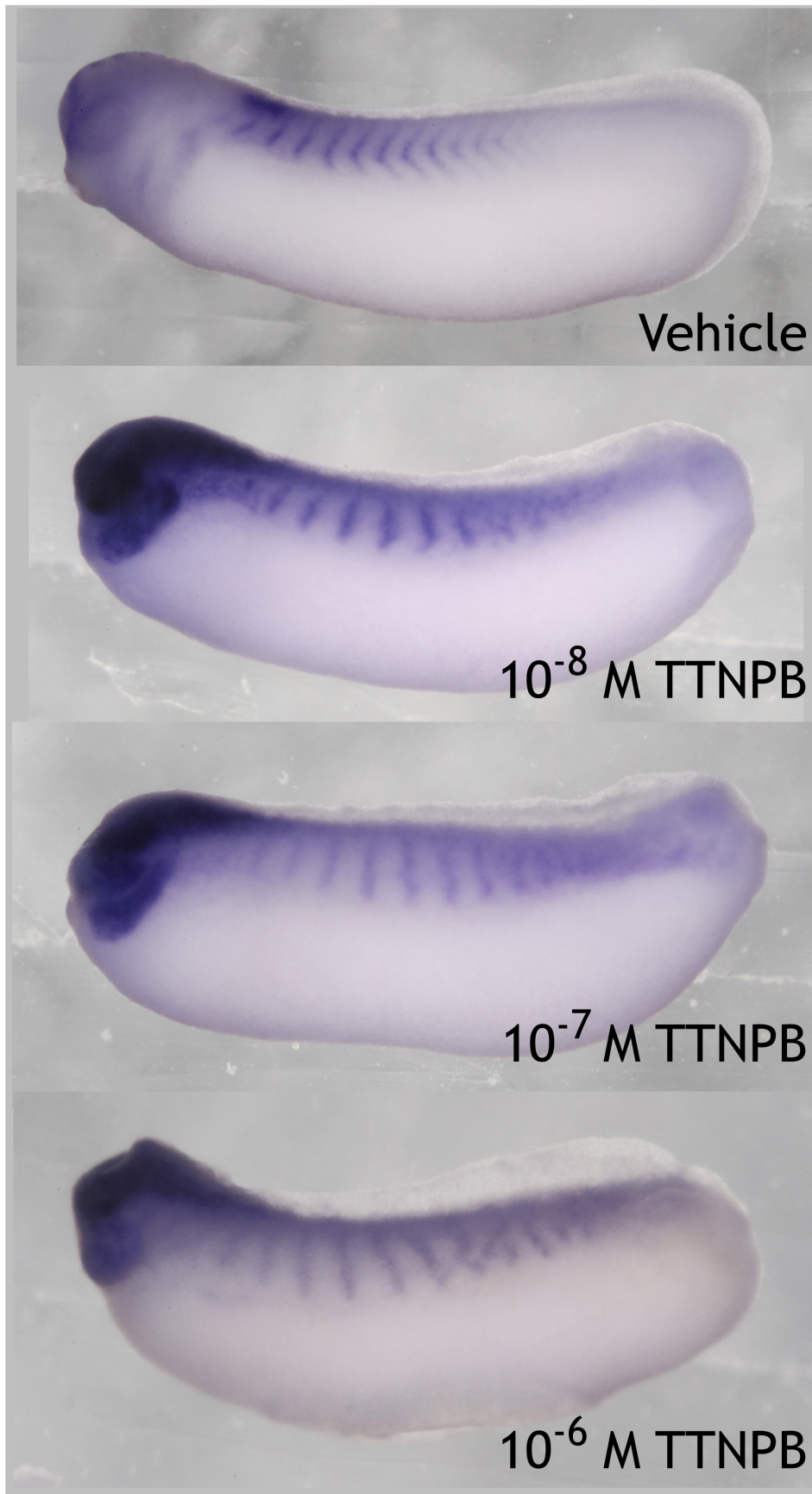
Supplemental Figure S2. Expression of *Rara1*, *Rara2*, *Rarβ1*, *Rarβ2*, *Rary1*, and *Rary2* across developmental time. QPCR showing *Rara1*, *Rara2*, *Rarβ1*, *Rarβ2*, *Rary1*, and *Rary2* gene expression over developmental time. Note that *Rary1* and *Rary2* were previously published in Janesick, et al., 2014, but shown here for comparison purposes. Error bars = S.E.M. The y-axis represents 2^{-ΔCt} values (adjusted for primer efficiency), normalized to reference gene, *Histone H4*. The y-axis values are comparable for all three graphs.



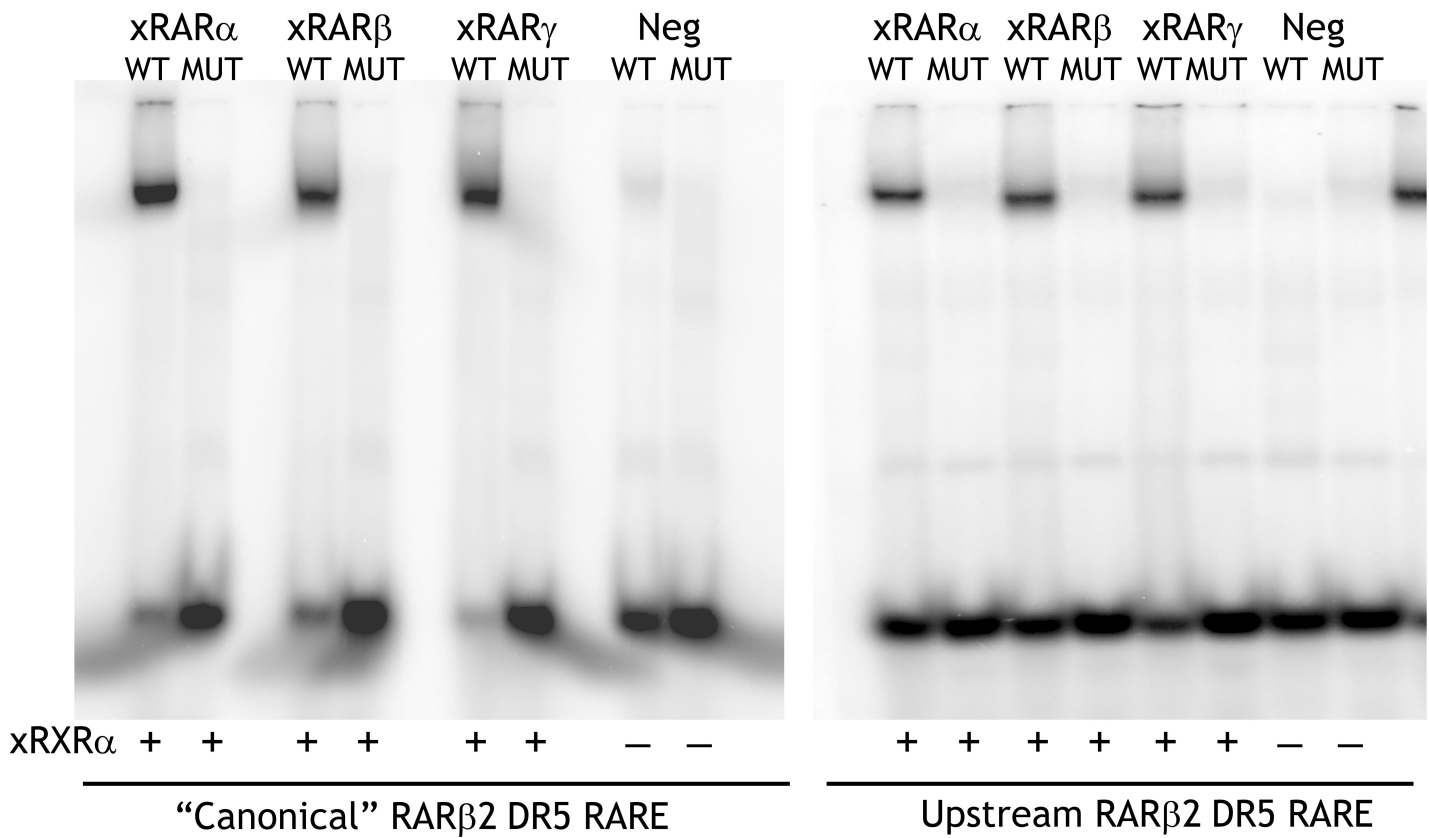
| | Expanded RAR β Conserved Region | | | |
|---------------|---------------------------------------|---------------------------------------------|-----------|--------------------------------------------|
| X. laevis | GGT | GATGTCAG | ACTG-GTGT | GGGTCA TTTGA AGGTTAG CA |
| X. tropicalis | GGT | GATGTCAG | ACTG-GTTT | GGGTCA TTTGA AGGTTAG CA |
| Human | GGT | GATGTCAG | ACT--AGTT | GGGTCA TTTGA AGGTTAG CA |
| Mouse | GGT | GATGTCAG | ACT--GGTT | GGGTCA TTTGA AGGTTAG CA |
| Turtle | GGT | GATGTCAG | ACTG-GTTT | GGGTCA TTTGA AGGTTAG CA |
| Chicken | GGT | GATGTCAG | AC---GCC | GGGTCA TTTGA AGGTTAG CA |
| Coelacanth | GGT | GATGTCAG | ACT--GGTT | GGGTCA TTTGA AGGTTAG CA |
| Medaka | GAT | GATGTCAG | ACAGCGGCT | GGGTCA TGTGA AGGGCAG CA |
| Fugu | AGT | GATGTC AA | --GCGCC | GGGTCA TTTGA AGGTCAG CA |
| Zebrafish | --- | ----- | ----- | GT GGGTCA TTGAG AGGTGA GGC |
| | | Upstream HS | | Upstream RARβ RARE |
| X. laevis | GCCTGGGAAG | GGTTTCATGGAAAGTTCAC | TCGCA | TAT-ATTA |
| X. tropicalis | GCCTGGGAAG | GGTTTCATGGAAAGTTCAC | TCGCA | TAT-ATTA |
| Human | GCCCGGGTAG | GGTTTCACCGAAAGTTCAC | TCGCA | TAT-ATTA |
| Mouse | GCCCGGGGAAG | GGTTTCACCGAAAGTTCAC | TCGCA | TAT-ATTA |
| Turtle | GCCTGGGAAG | GGTTTCATGGAAAGTTCAC | TCGCA | TAT-ATTA |
| Chicken | GCCTGGGAAG | GGTTTCACAGAAAGTTCAC | TCGCA | TAT-ATTA |
| Coelacanth | GCCTAGGAAG | GGTTTCATATAAAGTTCAC | TCGCA | TAT-ATTA |
| Medaka | GC--GGAGGC | GGTTTCACGGAGAGTTCAG | CCGCA | TAC-ATTA |
| Fugu | GCCTCGGAA | GGTTTCACGCAAAGTTCAC | TCGCA | TAT-ATTA |
| Zebrafish | TGACTGCTTCCAT | GGTTTCAGGAAAAGTTCAG | CCGCATA | ACATTA |
| Amphioxus | AGTTGGCCTG | GGTTTCAGTCAGAGTTCAG | CAAGTGA | ACTTTC |
| Ciona | AGACTGGATA | AGGTCA -TA-- GGGTCA | CAGTAAGCG | CCC |
| | | Canonical RARβ RARE | | |

TATA BOX

Supplemental Figure S3. *Rar β* contains highly conserved retinoic acid response elements (RAREs). Conserved DR5 RAREs and half sites found in the promoter of *Rar β* in chordate species. Exceptions: zebrafish RARE is found in *raraa* (RAR α); Ciona RARE is found downstream, in the first intron. Amphioxus and Ciona lack the upstream HS and upstream RARE. Abbreviations: HS = half site; C = canonical; DR5 = direct repeat 5.



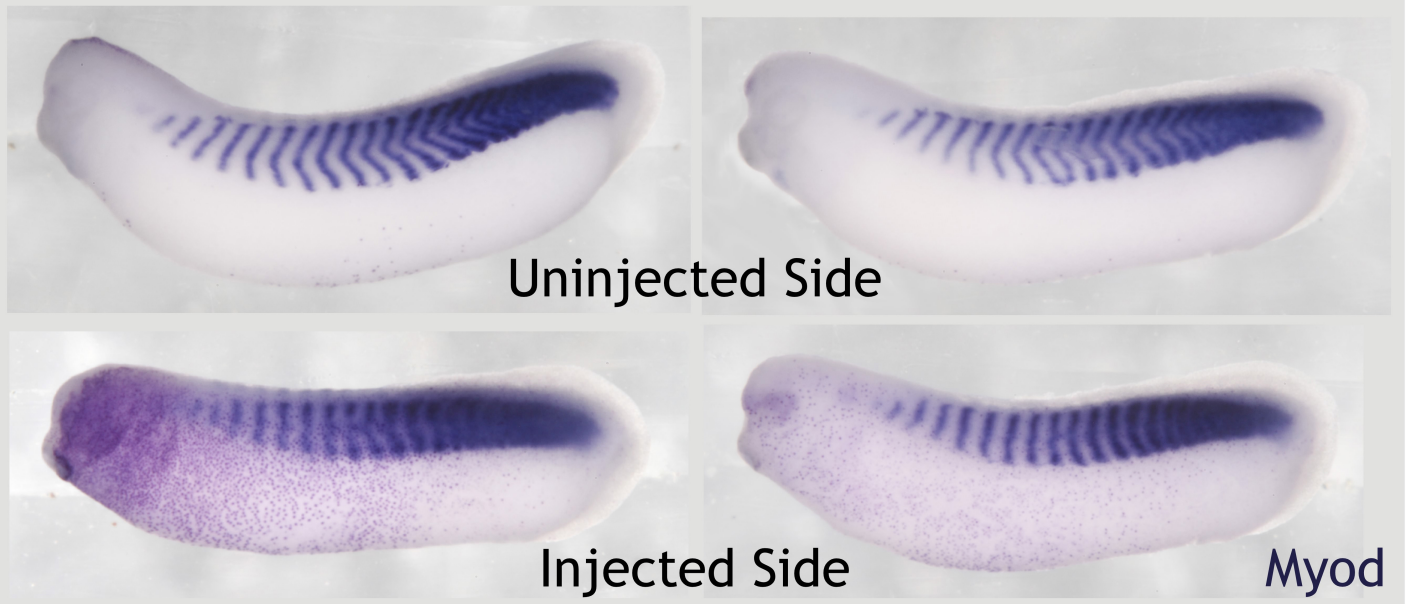
Supplemental Figure S4. *Rarb2* expression is significantly expanded by TTNPB. WISH from embryos treated at stage 6/7 with TTNPB or control vehicle (0.1% EtOH). Embryos are shown in lateral view at tailbud stage 26; anterior is on the left.



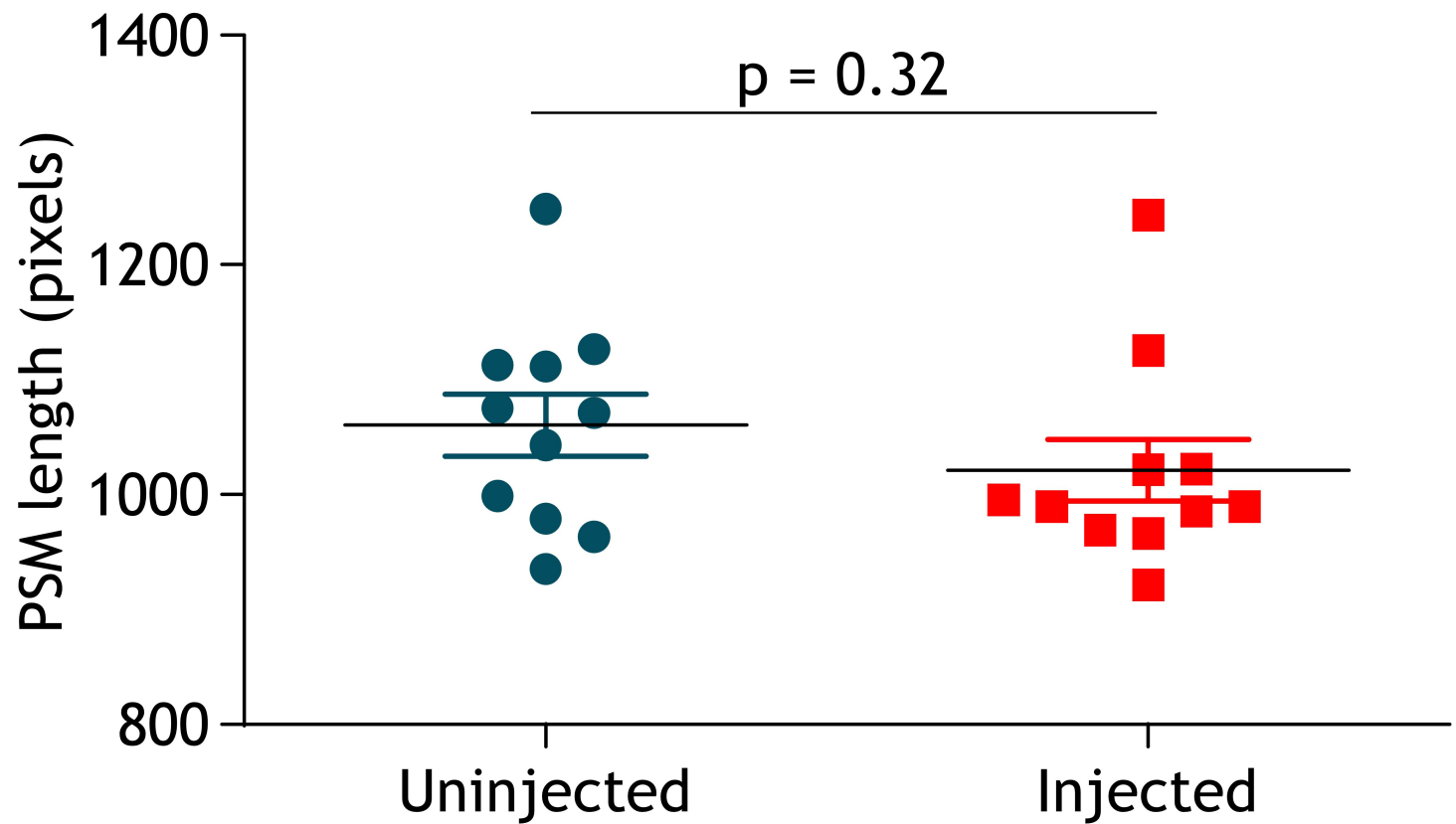
Supplemental Figure S5. Xenopus RARs are capable of binding the canonical and upstream *Rarβ2* direct repeat 5 (DR5) retinoic acid response elements (RAREs). Electrophoretic mobility shift assay with xRAR/xRXR heterodimers was conducted with wildtype and mutated RARE oligonucleotides (Supplemental material, Table S6). Negative control was the in vitro translation reaction, minus RNA.

Rarb2.L MO

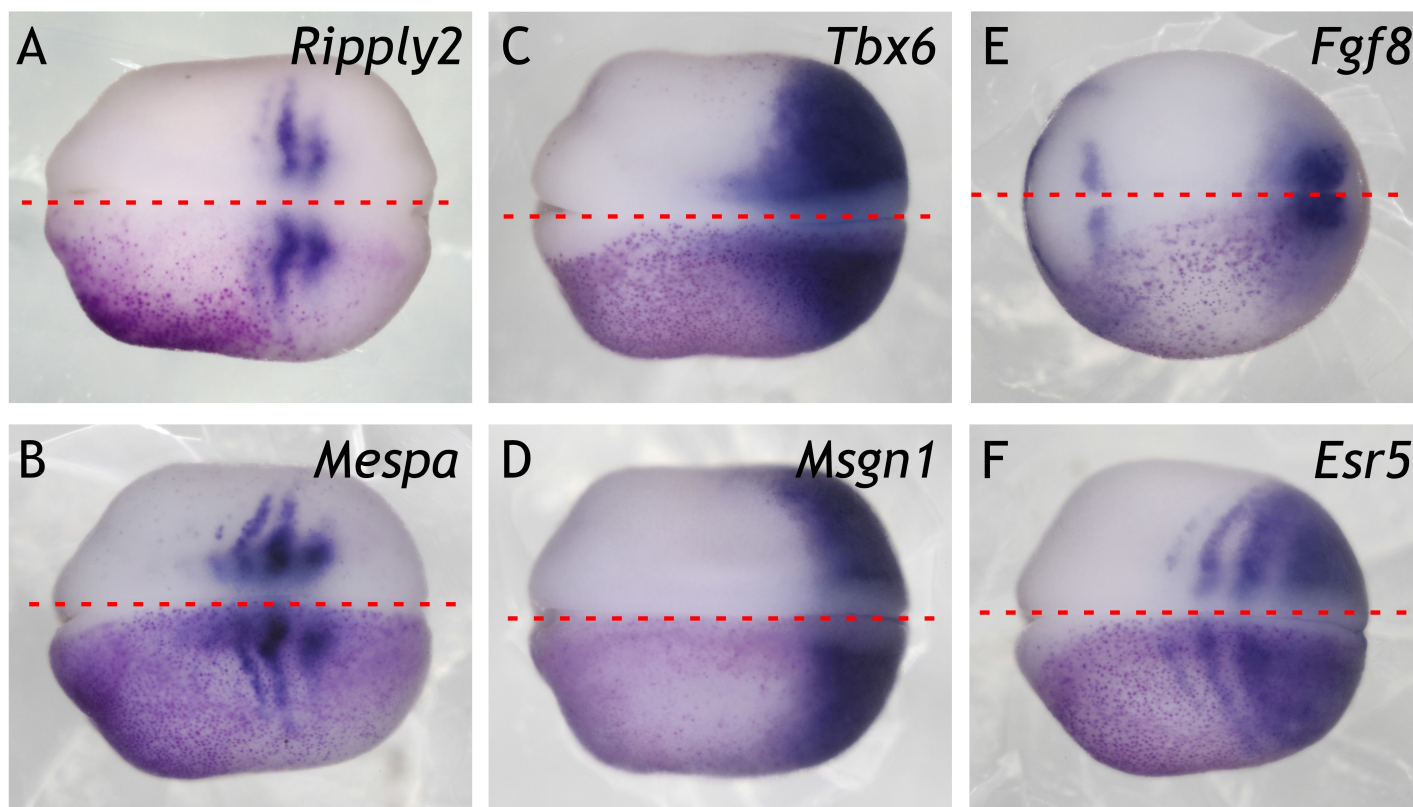
Rarb2.S MO



Supplemental Figure S6. Morpholinos targeted against either the .L or .S homeologs of *Rarβ2* result in the same phenotype. Embryos were microinjected unilaterally at 2- or 4-cell stage with 52 ng *Rarβ2.L* MO or 52 ng *Rarβ2.S* MO. Two lateral sides of the same embryo are shown at stage 26; anterior on the left. Injected side is indicated by magenta *β-gal* lineage tracer. *Rarβ2.L* MO or *Rarβ2.S* MO disrupt and disorganize the chevron-shaped somite morphology marked by *Myod*.



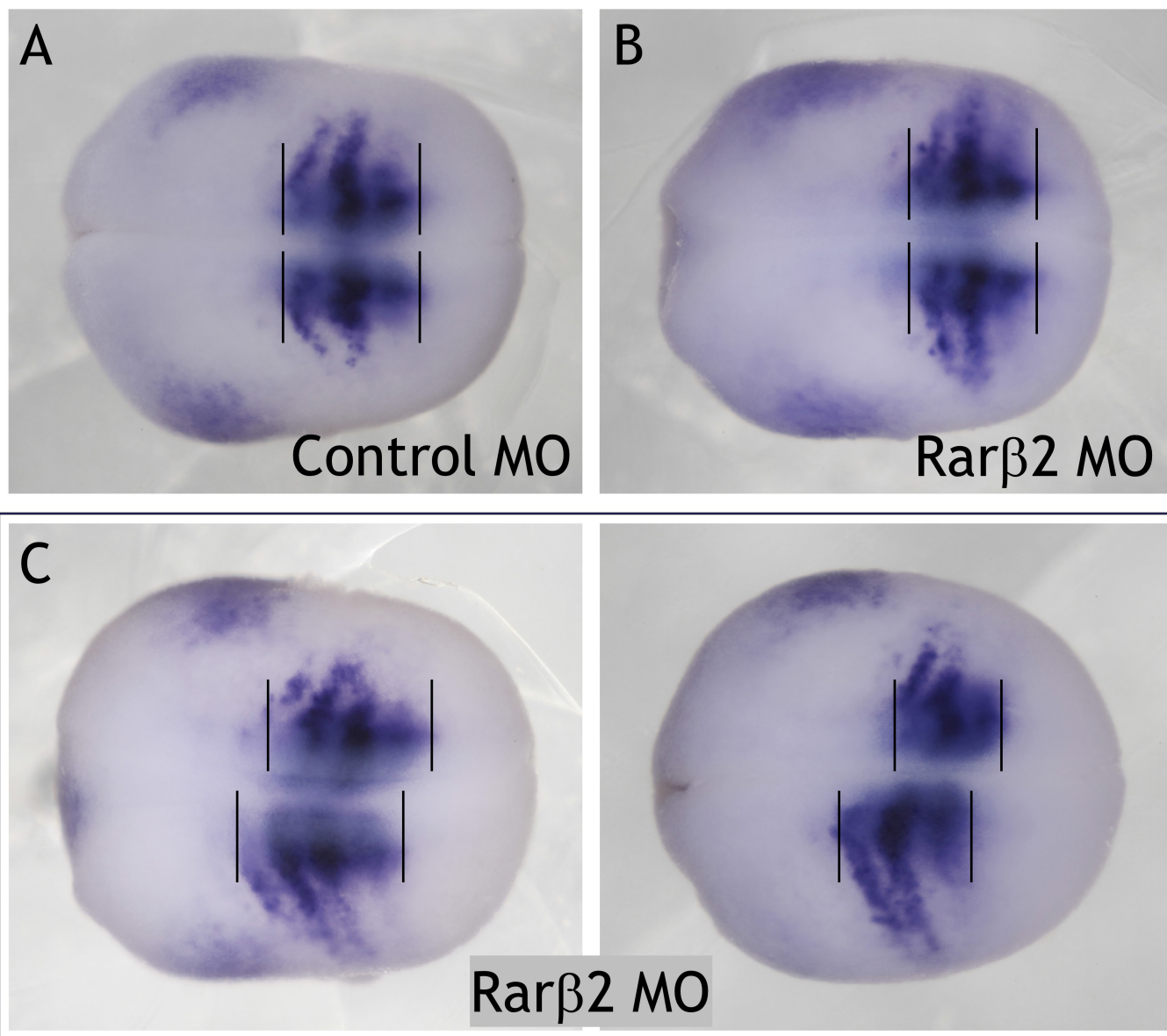
Supplemental Figure S7. Size of the unsegmented PSM is unchanged in *Rarβ2* MO-injected embryos. Embryos were microinjected unilaterally at 2- or 4-cell stage with 26 ng *Rarβ2.L* + 26 ng *Rarβ2.S* MOs do not alter the size of the PSM, as indicated by unsegmented *Myod* expression. PSM length is quantitated using ImageJ (units are distance in pixels); each data point represents one embryo. Statistics were conducted in GraphPad Prism v5 using a paired t-test.



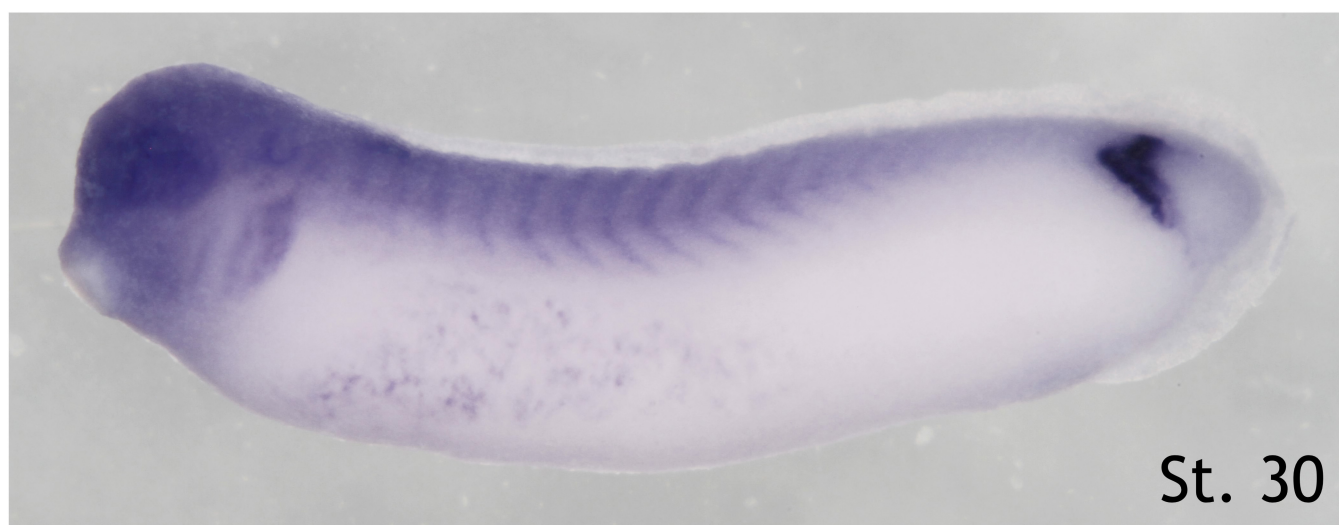
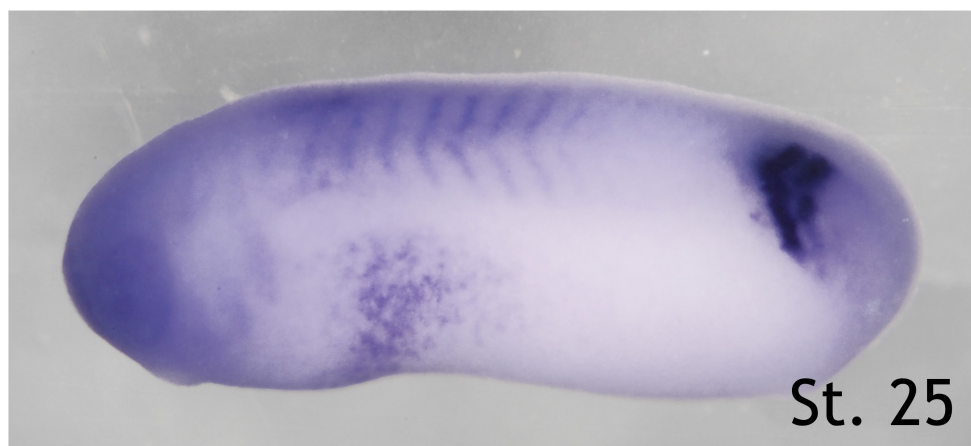
Supplemental Figure S8. Control MO-injected embryos corresponding to Figure 6.

(A-F) Embryos were injected unilaterally at 2- or 4-cell stage with 52 ng Control MO.

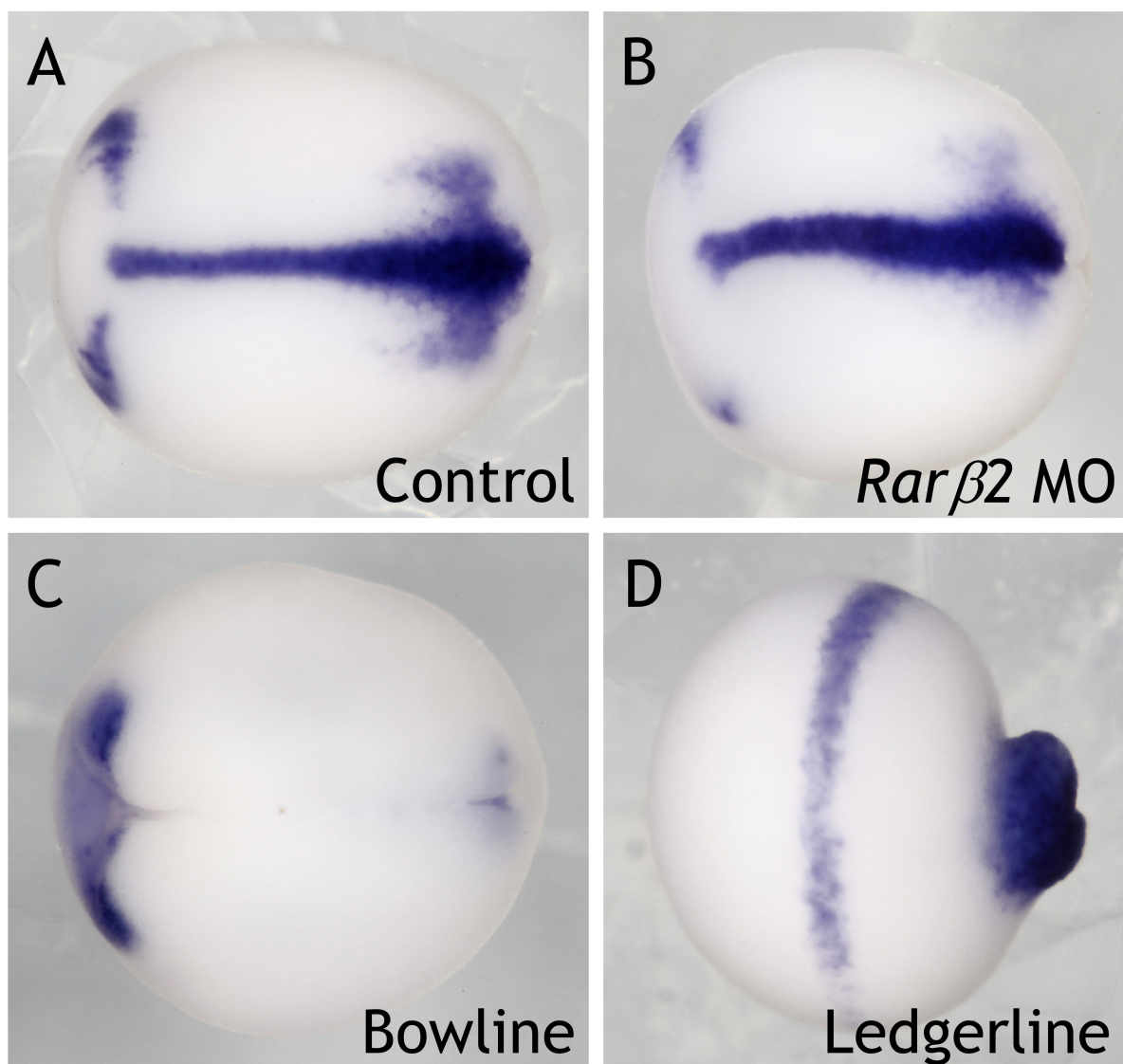
Injected side is indicated by magenta β-gal lineage tracer. Neurula stage embryos shown in dorsal view with anterior on left. Control MO does not alter expression of somitomere markers (A) *Ripply2* (13/15 embryos) and (B) *Mespa/Thyl2* (12/16). The expression domains of presomitic mesoderm markers *Tbx6* (C), *Msgn1* (D), *Fgf8* (E), and *Esr5* (F) are also unaltered (*Tbx6*: 16/17 embryos; *Msgn1*: 21/21; *Fgf8*: 16/18; *Esr5*: 19/20).



Supplemental Figure S9. Somite asymmetry is observed in *Rarβ2* MO-injected embryos. (A-C) Embryos were injected bilaterally at 2-cell stage with (A) 52 ng Control MO or (B, C) 26 ng *Rarβ2.1* MO + 26 ng *Rarβ2.2* MO. Neurula stage embryos shown in dorsal view with anterior on left. *Rarβ2* MOs resulted in either (B) normal somite symmetry (17/25 embryos) or (C) abnormal somite asymmetry (8/25). Control MO (A) showed normal somite symmetry (22/23)



Supplemental Figure S10. Double WISH of *Rarβ2* and *Ripply2*.

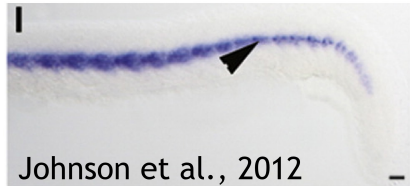


Supplemental Figure S11. Notochord (*Xnot*) defects observed in *Rarβ2* MO-injected and *Ripply2*-overexpression embryos. (A-D) Embryos were injected bilaterally at 2-cell stage with (A) 52 ng Control MO or 0.5 ng Control *mCherry* mRNA (one representative control shown here), (B) 26 ng *Rarβ2.1* MO + 26 ng *Rarβ2.2* MO, (C) 0.5 ng *Bowline* mRNA or (D) 0.5 ng *Ledgerline* mRNA. Neurula stage embryos shown in dorsal view with anterior on left. *Rarβ2* MOs resulted in a crooked notochord (10/19 embryos) and shorter body axis (19/19 embryos). *Bowline* overexpression eliminated *Xnot* expression (16/16 embryos) and *Ledgerline* created severe axial defects with diminished *Xnot* expression (23/24 embryos).

Zebrafish



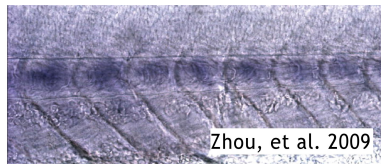
En1



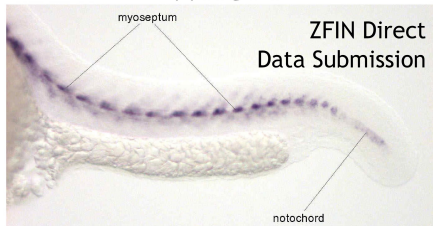
Cxcl12a



Plce1



Wnt11



Hhatl

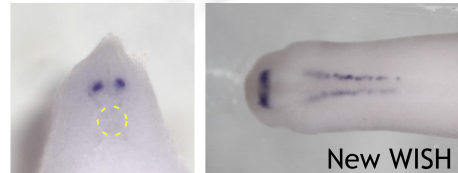
ZFIN Direct Data Submission



Xenopus



En1



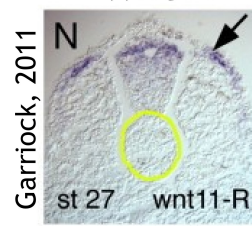
Cxcl12a

Probe designed.
No specific signal.

Plce1

No Xenbase data
Did not test because
FPKM was < 1

Wnt11



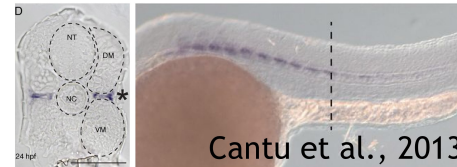
Hhatl



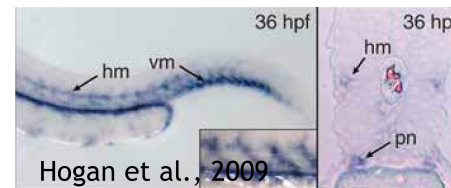
Zebrafish



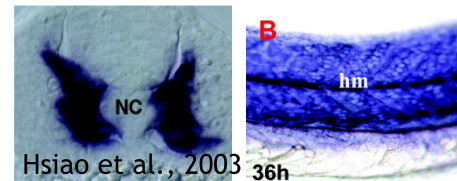
Notum



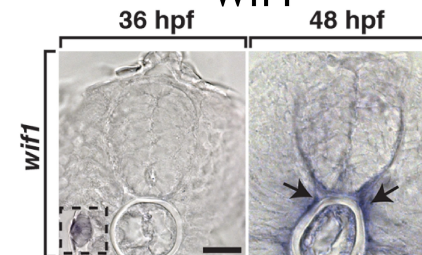
Ccbe1



Mybpc1



Wif1



Xenopus



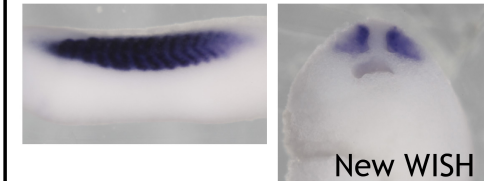
Notum



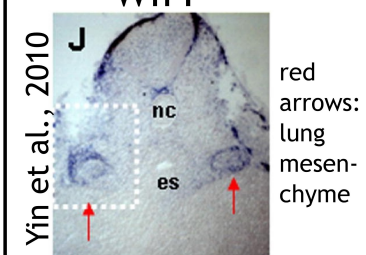
Ccbe1

No Xenbase data
Did not test because
FPKM was < 0.1

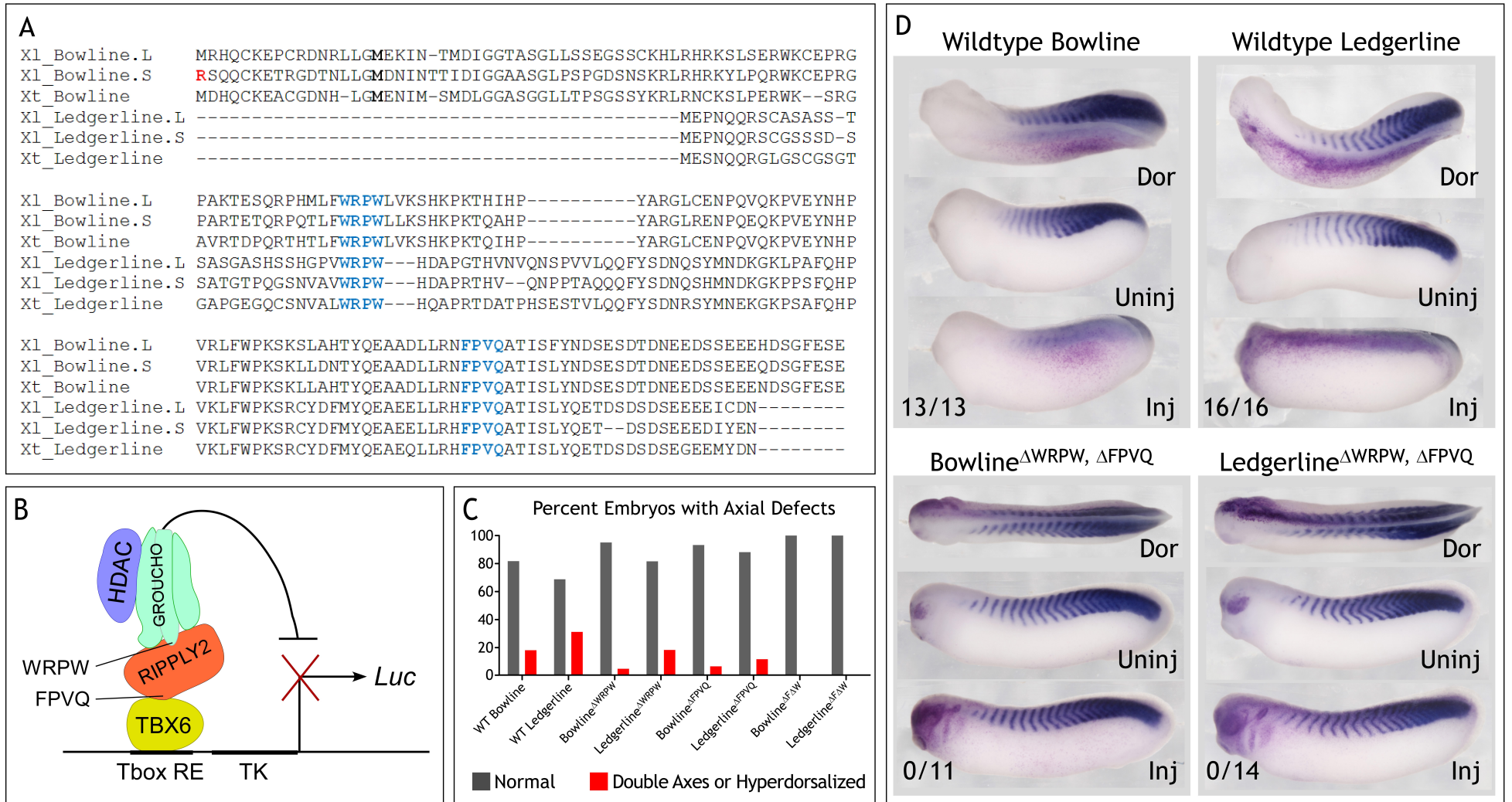
Mybpc1



Wif1



Supplemental Figure S12. Comparison of myoseptum and adaxial “pioneer” markers in zebrafish versus Xenopus. New WISH indicates that a probe was designed specifically for this paper, and was not published previously or available on Xenbase. FPKM = Fragments Per Kilobase of transcript per Million mapped reads (data not shown).



Supplemental Figure S13. (A) MAFFT multiple alignment of *Xenopus Ripply2* proteins Bowline and Ledgerline. Xl = *Xenopus laevis*; Xt = *Xenopus tropicalis*. All sequences were obtained from Xlv9.1 or Xtv9.0 genomes on Xenbase (Karpinka et al., 2014). **(B) Diagram of T-Box response element (RE) TK-luciferase (luc) reporter and *Ripply2* protein interactions.** The Brachyury palindromic element is present in two copies, preceding the TK minimal promoter and luciferase. **(C) Quantitation of axial defects due to *Ripply2* overexpression.** Embryos were microinjected unilaterally at 2- or 4-cell stage with 0.5 ng *Ripply2* wildtype or mutant mRNA (Δ WRPW = *Ripply2*^{WRPW→AAAA}; Δ FPVQ = *Ripply2*^{FPVQ→AAAA}; Δ WΔF = *Ripply2*^{WRPW→AAAA, FPVQ→AAAA}). **(D) *Ripply2* blurs and abolishes *Myod* expression in the somites.** Embryos were microinjected unilaterally at 2- or 4-cell stage with 0.5 ng *Ripply2* wildtype or mutant mRNA. Injected side is indicated by magenta β -gal lineage tracer. Embryos are shown in lateral view at stage 26; anterior on the left. Single mutant mRNA not pictured, but scored for *Myod* blurring and knockdown: *Bowline*^{ΔWRPW} (3/13 embryos); *Ledgerline*^{ΔWRPW} (18/18); *Bowline*^{ΔFPVQ} (4/14 blurred, 4/14 disorganized); *Ledgerline*^{ΔFPVQ} (2/22)

Supplemental Table S1 (Morpholinos)

| MO | Sequence (5'→3') |
|------------------|-----------------------------------|
| <i>Rarβ2.S</i> | AGC TAA TAT TGT GTA TAG GGG GGG A |
| <i>Rarβ2.L</i> | CTT TAC AGA ATA TCA GCG AAA GTG C |
| <i>Rarγ1.L/S</i> | GCT GTT TGC CAT TGC CTT GTT CTA |
| <i>Rarγ2.L/S</i> | TTC CAT GCA GTC ATA CAT TTT GGG |
| <i>Rara1</i> | GCT CCA AAC GCA CTT CTA CTC CCT C |
| <i>Rara2.S</i> | CTG AAA TCC AAA CTG ACC ATA GAG T |
| <i>Rara2.L</i> | ATC CAA AGG AAG GTG AGT GTG TGT G |

Supplemental Table S2 (Probe Design)

Probes with T7 Adapters

| Primer | Sequence (5'→3') |
|---------------------------|-------------------------------------------------------------|
| F (<i>Rarb1</i>): | GAT AAT ACA TCA TTC TTT GCC TCC CTG G |
| R (<i>Rarb1</i>): | taa tac gac tca cta tag ggC TCT GGG TTT CGA TGG TTG CTG |
| F (<i>Rarb2</i>): | CAG GAA TTT AGA TGC ATT TTG CCT GG |
| R (<i>Rarb2</i>): | taa tac gac tca cta tag ggC CAT TCT GTC TGT GCC AAT CCA C |
| F (<i>Rarb2-Sense</i>): | taa tac gac tca cta tag ggA GGA ATT TAG ATG CAT TTT GCC TGG |
| R (<i>Rarb2-Sense</i>): | CCA TTC TGT CTG TGC CAA TCC AC |
| F (<i>Ripply2</i>): | GCA AGT GGT TTG CCA AGT CC |
| R (<i>Ripply2</i>): | taa tac gac tca cta tag ggT CAA ATC CAG AGT CTT GTT CCT CC |
| F (<i>Mespa/Thyl2</i>): | ACA CTT AAA CCA GAG TCT TTC ACC T |
| R (<i>Mespa/Thyl2</i>): | taa tac gac tca cta tag ggA TCT GAA GCT TTG CCT TCA GTG G |
| F (<i>Mesogenin</i>): | AAT GGA AGA GGA CTA TGC CTT GAG |
| R (<i>Mesogenin</i>): | taa tac gac tca cta tag ggT CTT GGA GCA CTG GAG AAG GT |
| F (<i>Tbx6</i>): | GGC ACC TCC TAC ACG ATG AGA C |
| R (<i>Tbx6</i>): | taa tac gac tca cta tag ggC TCC TCT TCC TGT TCC TGT TCC A |
| F (<i>MyoD</i>): | CAC TGC GGG ACA TGG AAG TC |
| R (<i>MyoD</i>): | taa tac gac tca cta tag ggG TAT TGC TGG GAG AAG GGA TGG T |
| F (<i>Esr5</i>): | TCC AGG AAG ATC CTC AAA CCG |
| R (<i>Esr5</i>): | taa tac gac tca cta tag ggC TCC ATA TGT ACA ATG GCG GCT G |
| F (<i>Cxcl12</i>): | GCT CTG CTC TCC ATC CTG CT |
| R (<i>Cxcl12</i>): | taa tac gac tca cta tag ggC TTT CTC CAG GTA CTC C |
| F (<i>Mybpc1</i>): | GGT TGA AAG GCA AAT GGA TGG AC |
| R (<i>Mybpc1</i>): | taa tac gac tca cta tag ggA GGT TCT CTG ACA AAC AGC |
| F (<i>En1</i>): | TCT TCA TAG ACA ACA TTC TCC GGC |
| R (<i>En1</i>): | taa tac gac tca cta tag ggT GGT TGT ACA GTC CCT GAG C |
| F (<i>Tbx3</i>): | TGT ATA TCC ATC CAG ACA GCC CG |
| R (<i>Tbx3</i>): | taa tac gac tca cta tag ggT AGA TTC GCC TGT GTC CG |

Supplemental Table S3 (QPCR)

| Primer | Sequence (5'→3') |
|--------------------------|-----------------------------------|
| F (<i>xRARα1</i>): | CCA CAT ATG TTG GGG GGT ATG TC |
| R (<i>xRARα1</i>): | GAT TCT GGG GAG CGG TGG T |
| F (<i>xRARα2</i>): | CCA CTC AAT TGA GAC TCA GAG CAC |
| R (<i>xRARα2</i>): | CTC TTG TCC TGA CAC ACA AAG CA |
| F (<i>xRARβ1</i>): | TTT CCT CCT GTC ATT GGT GGA CTC |
| R (<i>xRARβ1</i>): | GCT CTG GGT TTC GAT GGT TGC |
| F (<i>xRARβ2</i>): | CAA ATG CTG GAT TTC TAC ACT GCG |
| R (<i>xRARβ2</i>): | GTG TTG CCA TTC TGT CTG TGC C |
| F (<i>xRARγ1</i>): | AGA ACA AGG CAA TGG CAA ACA G |
| R (<i>xRARγ1</i>): | GCA AGT ACT TCA AAT GGT GGA GAT C |
| F (<i>xRARγ2</i>): | GTA GAA ACA CAA AGT ACC AGC TCG |
| R (<i>xRARγ2</i>): | CCG TAG TGA TAA CCT GAA GAC TTG T |
| F (<i>Histone H4</i>): | GAT AAC ATC CAG GGC ATC AC |
| R (<i>Histone H4</i>): | TAA CCT CCG AAT CCG TAC AG |
| F (<i>Eef1a1</i>): | CAT CTC GCC CAA CCG ATA AGC |
| R (<i>Eef1a1</i>): | TTT AAT GAC ACC AGT CTC CAC ACG |

Supplemental Table S4 (pCDG1 Expression Constructs, *Ripply2* Two-Fragment PCR)

| Primer | Sequence (5'→3') |
|---------------------------------------|------------------------------------------------------------|
| F (pCDG1- <i>xTbx6</i>): | cag ata cca tgg AAT ACC ACT CTG AGC TCT TCC AGC AGT AT |
| R (pCDG1- <i>xTbx6</i>): | act agt gga tcc TTA CTA TCA CAT CCA GCC CCC C |
| F (pCDG1- <i>xTbx3</i>): | cag ata cca tgg ATT TAC CCA TGA GAG ATC CAG TAA TTT CAG G |
| R (pCDG1- <i>xTbx3</i>): | act agt gga tcc TTA TCA GTC AGG GGA ACC GCT C |
| F (pCDG1- <i>Ledgerline</i>): | cag ata cca tgg AGC CGA ATC AAC AGC GGA G |
| R (pCDG1- <i>Ledgerline</i>): | act agt gga tcc TTA ATT TTC ATA AAT GTC TTC CTC TTC AG |
| F (pCDG1- <i>Bowline</i>): | cag ata cca tgg ACA ACA TTA ACA CTA CTA TTG ACA TTT |
| R (pCDG1- <i>Bowline</i>): | act agt gga tcc TTA TTC AGA TTC AAA TCC AGA GTC TTG T |
| F (pCDG1- <i>Ledgerline_WRPW_B</i>): | ATG TGC AGC TGC AGC CAC TGC CAC ATT GCT GCC CT |
| R (pCDG1- <i>Ledgerline_WRPW_C</i>): | GTG GCT GCA GCTG CAC ATG ATG CCC CTA GGA CCC AT |
| F (pCDG1- <i>Ledgerline_FPVQ_B</i>): | AGC TGC AGC TGC AGC ATG TCT CAA TAA TTC CTC GGC TTC CT |
| R (pCDG1- <i>Ledgerline_FPVQ_C</i>): | ACA TGC TGC AGC TGC AGC TAC AAT ATC TCT TTA CCA GGA GAC AG |
| F (pCDG1- <i>Bowline_WRPW_B</i>): | AAA GTG CAG CTG CAG CGA ACA ATG TTT GAG GTC TCT GTG TTT C |
| R (pCDG1- <i>Bowline_WRPW_C</i>): | GTT CGC TGC AGC TGC ACT TTT GAA ATC CCA TAA ACC AAA GAC CC |
| F (pCDG1- <i>Bowline_FPVQ_B</i>): | GGC TGC AGC TGC AGC GTT TCT AAG CAA ATC TGC TGC CT |
| R (pCDG1- <i>Bowline_FPVQ_C</i>): | AAC GCT GCA GCT GCA GCC ACA ATA TCT CTC TAC AAT GAC TC |

Supplemental Table S5 (β -RARE Two-Fragment PCR)

| Primer | Sequence (5'→3') |
|----------------------------------|------------------------------------------------------------------------------|
| F (pGL3-RAR β 2.2_A) | ccc ggg ctc gag GCT CGC TGC TAG TCT TTA AGC TG |
| R (RAR β 2.2_Mut_C-DR5_B) | TGC GAG TGT TCT TTC CAT GTT CCC TTC CCA GGC TGC TAA CC |
| F (RAR β 2.2_Mut_C-DR5_C) | CTG GGA AGG GAA CAT GGA AAG AAC ACT CGC ATA TAT TAG GC |
| R (RAR β 2.2_Mut_Up-DR5_B) | CAG GCT GCT ATT CTT CAA ATG TTC CAC ACC AGT CTG ACA TCA C |
| F (RAR β 2.2_Mut_Up-DR5_C) | CTG GTG TGG AAC ATT TGA AGA ATA GCA GCC TGG GAA GGG TTC ATG GA |
| R (RAR β 2.2_Mut_HS_B) | TGA CCC ACA CCA GTC TGT TAT CAC CAA CTC CCA GGA TTC TCA |
| F (RAR β 2.2_Mut_HS_C) | CTG GGA GTT GGT GAT AAC AGA CTG GTG TGG GTC ATT TGA AGG |
| R (pGL3-RAR β 2.2_D) | aat gcc aag ctt CAG CTC ACT TCC TAC TAC TTG TGT |

Supplemental Table S6 (β -RARE EMSA)

| Primer | Sequence (5'→3') |
|--------------------------|-----------------------------|
| F (EMSA_RARE_C-DR5) | GGAAGGGTTCATGGAAAGTTCACTCGC |
| R (EMSA_RARE_C-DR5) | GCGAGTGAACCTTCCATGAACCCTTCC |
| F (EMSA_RARE_Mut_C-DR5) | GGAAGGGAACATGGAAAGAACACTCGC |
| R (EMSA_RARE_Mut_C-DR5) | GCGAGTGTTCTTCCATGTTCCCTTCC |
| F (EMSA_RARE_Up-DR5) | GGTGTGGGTCATTTGAAGGTTAGCAGC |
| R (EMSA_RARE_Up-DR5) | GCTGCTAACCTTCAAATGACCCACACC |
| F (EMSA_RARE_Mut_Up-DR5) | GGTGTGGAACATTTGAAGAATAGCAGC |
| R (EMSA_RARE_Mut_Up-DR5) | GCTGCTATTCTTCAAATGTTCCACACC |